

See discussions, stats, and author profiles for this publication at: <https://www.researchgate.net/publication/23134312>

# Metallodynamers: Neutral Double-Dynamic Metallosupramolecular Polymers

ARTICLE *in* CHEMISTRY - AN ASIAN JOURNAL · SEPTEMBER 2008

Impact Factor: 4.59 · DOI: 10.1002/asia.200800101 · Source: PubMed

---

CITATIONS

13

---

READS

15

3 AUTHORS, INCLUDING:



Cheuk-Fai Chow

The Hong Kong Institute of Education

42 PUBLICATIONS 687 CITATIONS

SEE PROFILE

# Metallodyn timers: Neutral Double-Dynamic Metallosupramolecular Polymers

Cheuk-Fai Chow,<sup>[a, c]</sup> Shunsuke Fujii,<sup>[a, b]</sup> and Jean-Marie Lehn<sup>\*[a]</sup>

*Dedicated to Professor Ryoji Noyori on the occasion of his 70th birthday*

**Abstract:** Nine neutral dynamic metallosupramolecular polymers (metallodyn timers) based on acyl hydrazone derived metal coordination centers ( $\text{Co}^{2+}$ ,  $\text{Ni}^{2+}$ ,  $\text{Zn}^{2+}$ , and  $\text{Cd}^{2+}$ ) were generated through self-assembly polymerization. These are linear coordination polymers with specific optical and mechanical properties. Monomer selection was found to take place in a mixture of

subcomponents (carboxyaldehydes and bisacyl hydrazides) driven by hexacoordination to a specific metal ion. Most importantly, the metallodyn timers were

**Keywords:** ligand exchange • polymerization • polymers • self-assembly • supramolecular chemistry

found to modify their constitution by exchanging and reshuffling their components with another metallodyner through ligand exchange at the metal coordination site in solution as well as in the neat phase. As a result, the materials undergo remarkable changes in both their mechanical and optical properties.

## Introduction

Supramolecular chemistry is about dynamism.<sup>[1]</sup> The interactions that connect the molecules of a supramolecular entity are easily broken and reformed, thus allowing supramolecular species to modify their constitution readily by incorporating, exchanging, and reorganizing their components. This dynamic form of chemistry concerns the constitution of the chemical object itself. When it is imported into molecular chemistry by the introduction of reversible bonds, dynamic covalent chemistry is attained,<sup>[2]</sup> which, together with supramolecular chemistry, defines constitutional dynamic chemistry (CDC)<sup>[1b,c]</sup> on both the molecular/covalent and the supramolecular/noncovalent levels. The introduction of CDC into

materials science, in particular, polymer chemistry, leads to dynamic polymers: dynimers that are both supramolecular<sup>[1,3]</sup> and molecular<sup>[1,2,3e]</sup> in nature.

Dynimers are particularly interesting because both microscopic and macroscopic properties of the polymeric entities can be rationally altered and tuned after polymerization. Dynimers may be defined as constitutional dynamic polymers, that is, polymeric entities whose monomeric components are linked through reversible connections and have the capacity to modify their constitution by incorporation, exchange, and reshuffling of their components.<sup>[1b,c,3b,e]</sup> Traditionally, the primary focus of polymer chemistry has been to avoid constitutional exchange reactions and to produce chemically well-defined, unique polymers, in particular, for industry.<sup>[4]</sup> Dynimers, by taking advantage of their ability to modify components through breaking and reforming their connections, provide a means for developing new materials that exhibit unusual properties.<sup>[3,5]</sup> Dynimers based on reversible covalent bonds<sup>[3e,5]</sup> were recently shown to undergo constitutional exchange reactions and transformation of macroscopic properties in solution as well as in neat polymer films.<sup>[5h,j]</sup> Such constitutional exchange may also occur in a special class of supramolecular dynimers, coordination polymers,<sup>[6]</sup> in which the monomeric components are ligand molecules linked through metal-ion coordination. As kinetically labile metal-ligand interactions are by nature dynamic, the coordinative bonding can dissociate and associate under

[a] Dr. C.-F. Chow, S. Fujii, Prof. Dr. J.-M. Lehn  
Institut de Science et d'Ingénierie Supramoléculaires (ISIS)  
Université Louis Pasteur  
8 Allée Gaspard Monge, BP 70028, 67083, Strasbourg (France)  
Fax: (+33) 390 425 140  
E-mail: lehn@isis-ulp.org

[b] S. Fujii  
R&D Center, Mitsui Chemical Inc.  
580-32 Nagaura, Sodegaura, Chiba 299-0265 (Japan)

[c] Dr. C.-F. Chow  
Current address: Department of Chemistry  
The University of Hong Kong, Pokfulam Road  
Hong Kong (Hong Kong SAR, China)

the influence of chemical and physical triggers.<sup>[7]</sup> Therefore, these coordination polymers may be defined as dynamic metallosupramolecular entities, or metallohydnamers.<sup>[7]</sup> Coordination polymers have drawn much attention in polymer science in recent times because properties such as charge, color, luminescence, magnetism, macroscopic morphology, and kinetic lability can in principle be tuned with the appropriate combination of ligands and metal ions.<sup>[6]</sup> Although most of them are either cationic or anionic,<sup>[6]</sup> it would be of much interest to assemble monomeric ligands and metal ions in such a way that they generate neutral coordination polymers,<sup>[7]</sup> which can ultimately be used to blend into conventional neutral polymers. Furthermore, the coordination site itself may be self-assembled from a set of subunits driven by metal-ion binding and with subunit selection, as was shown to occur in the formation of grid-type metallosupramolecular architecture.<sup>[8]</sup> Such coordination-site self-assembly has been implemented in the formation of coordination polymers.<sup>[7]</sup>

The present report describes the self-assembly and properties of coordination polymers based on neutral coordination centers and that display both metallosupramolecular and molecular covalent dynamics. We also report their dynamic constitutional modification through ligand exchange at the metal coordination site with another dynamic polymer in the neat phase (without any catalyst) as well as the resulting acquisition of novel functional properties. These coordination polymers combine a particularly broad range of features: 1) a metallosupramolecular linkage through metal-ion coordination; 2) self-assembly of the connection sites from ligand subunits; 3) neutral/charged interchange through NH ionization or NR substitution with concomitant organophilic/hydrophilic behavior; 4) constitutional dynamics modulated by the nature of the coordination center, thus allowing coordination-site reshuffling by exchange of either ligand or metal ion; 5) orthogonal double dynamics involving both reversible coordination and reversible covalent-bond (imine) formation; 6) control of initiation and polymerization through either metal-ion coordination or imine condensation or both; 7) potential combinatorial monomer selection in a mixture of monomers by tetra-, penta-, or hexacoordination driven by specific metal ions; and 8) dynamic modulation of functional features such as optical or mechanical properties through component recombination (Figure 1).

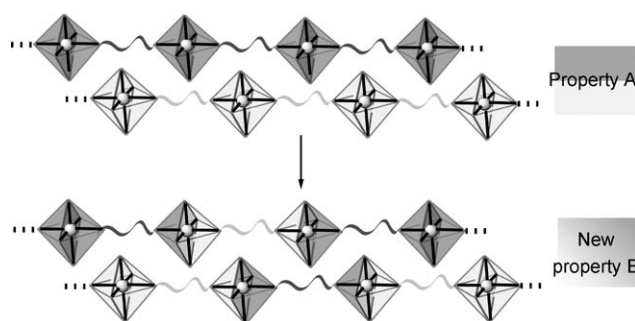


Figure 1. Schematic representation of the transformation of properties that result from constitutional metal-ligand exchange reactions in metallohydnamers.

## Results and Discussion

### Synthesis and Characterization of Ligand Subunits, Free Ligands, and Model Complexes

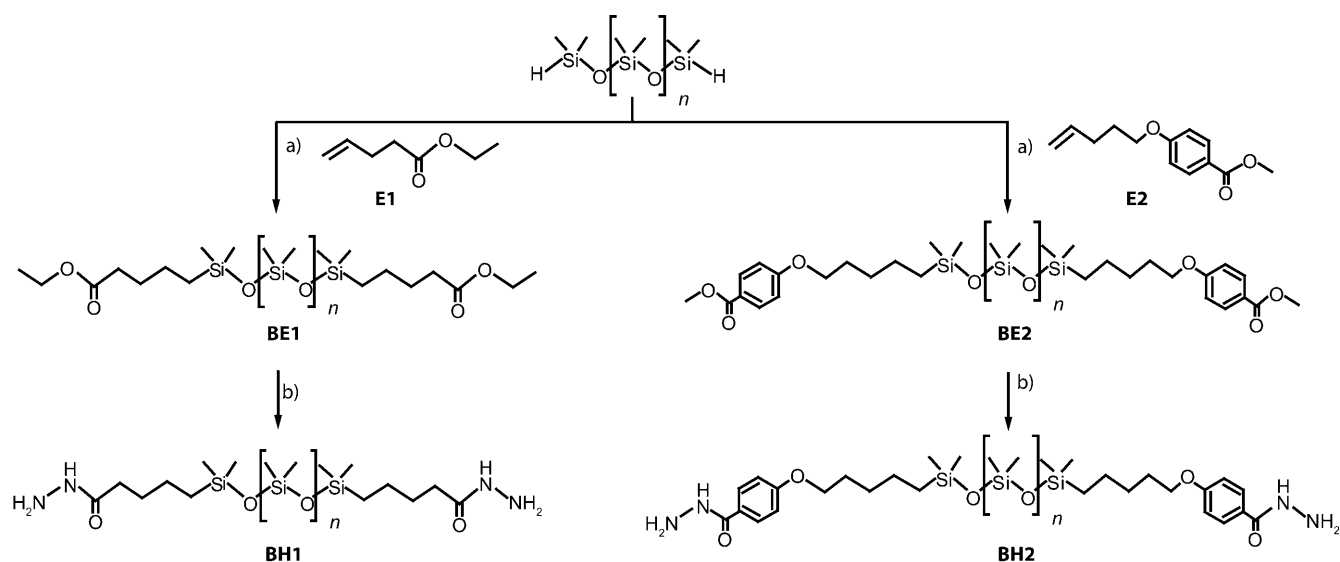
To obtain reference data for the study of the dynamic metallosupramolecular polymers, we first synthesized a series of ligand subunits: carboxaldehydes and bisacyl hydrazides, free acyl hydrazone ligands, and neutral model metal complexes, so as to characterize their spectroscopic properties and for comparison with metallosupramolecular polymers. Pyridine-2-carboxyaldehyde (Py2al), quinoline-2-carboxyaldehyde (Qui2al), and 5-decyloxy-pyridine-2-carboxyaldehyde (Py2alC<sub>10</sub>) were used as core aldehyde subcomponents. Py2alC<sub>10</sub> was synthesized from the nucleophilic substitution reaction of 1-iododecane with 5-hydroxypyridine-2-carboxyaldehyde in the presence of K<sub>2</sub>CO<sub>3</sub> in anhydrous *N,N*-dimethylformamide (DMF) as pale-yellow solids. The bisacyl hydrazide subcomponents **BH1** and **BH2** were obtained as oily materials by treating the hydride-terminated polydimethylsiloxane with corresponding alkene-terminated methyl or ethyl esters in the presence of the Karstedt catalyst, followed by treatment with hydrazine monohydrate in ethanol to convert the ester group into an acyl hydrazide (Scheme 1). The free acyl hydrazone ligands **L1–L6** were obtained by condensation of the corresponding aldehyde and acyl hydrazide (Scheme 2).

Neutral coordination centers may be obtained by using coordination subunits with ionizable sites. This is the case for the ionizable analogues of the tridentate terpyridine group<sup>[9]</sup> based on pyridyl hydrazone<sup>[10]</sup> and acyl hydrazone<sup>[11]</sup> units, which incorporate an N–H site that undergoes acidification and facile ionization upon binding of a metal ion.<sup>[14]</sup> The neutral model complex **1** (Figure 2) was formed by a self-assembly reaction by stirring 2 equivalents of Py2al and 4-chlorobenzoic hydrazide with 1 equivalent of Zn(SO<sub>4</sub>)·7H<sub>2</sub>O in the presence of Na<sub>2</sub>CO<sub>3</sub> at room temperature. A perspective view of the crystal structure with atom labeling is shown in Figure 2.<sup>[12]</sup> The coordination geometry of the Zn<sup>II</sup> center is a distorted octahedron with the two tridentate ligands lying almost perpendicular to each other. The dihedral angle between the mean planes defined by O1–N1–N2–N3 and O2–N4–N5–N6 is 94.6°. Deprotonation

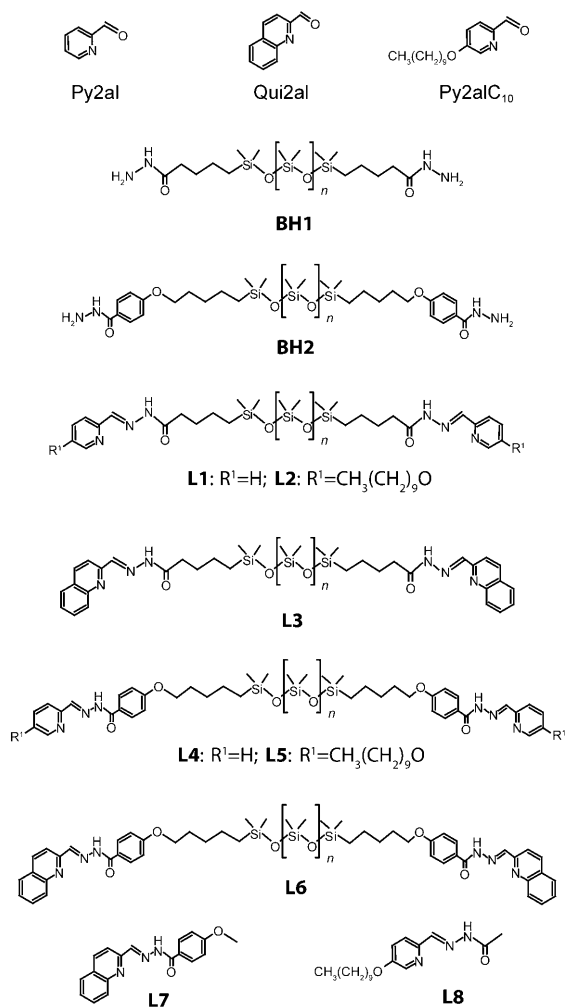
### Abstract in Chinese:

摘要:

酰肼衍生物与钴(II), 镍(II), 锌(II)以及镉(II)金属配位中心, 通过自组装聚合, 得到九个中性的动态金属超分子聚合物 (metallohydnamer)。这些线型配位聚合物具有特殊的光学和力学性质。当体系中存在多种芳香醛、酰肼组分时, 通过金属离子的六配位作用诱导, 可以使特定的组分发生反应。并且, 在溶液或无溶液体系中, 这些动态金属超分子聚合物能够与其它的动态金属超分子聚合物通过配体交换发生结构改变, 从而使材料的力学和光学性质发生明显变化。



Scheme 1. Synthetic scheme for the preparation of the bisacyl hydrazide subunits **BH1** and **BH2**. Reagents: a) Hydride-terminated polydimethylsiloxane (10 mmol), alkene-terminated ester **E1** or **E2** (24 mmol), and Karstedt catalyst (4 drops) in toluene (50 mL); b) **BE1** or **BE2** (10 mmol) and hydrazine monohydrate (200 mmol) in ethanol (15 mL).  $n \approx 13$  for all the siloxanes.



Scheme 2. Structures of the aldehyde, hydrazine, and hydrazone subcomponents ( $n \approx 13$ ).

of the acidic protons from the amide moieties in **1** results in a neutral complex. The neutral heteroligand complex **2** was formed by stirring equal amounts of presynthesized acyl hydrazone ligands **L7** and **L8** as well as  $\text{Zn}(\text{SO}_4) \cdot 7\text{H}_2\text{O}$  in the presence of  $\text{Na}_2\text{CO}_3$  at room temperature. Nine other neutral homoligand model complexes **3–11** were also obtained by a procedure similar to that for complex **1**: one-pot reaction of an acyl hydrazide (octyloic hydrazide or 4-methoxybenzhydrazide) with a carboxaldehyde (Py2al, Py2alC<sub>10</sub>, or Qui2al) and a  $\text{Co}^{\text{II}}$ ,  $\text{Ni}^{\text{II}}$ ,  $\text{Zn}^{\text{II}}$ , or  $\text{Cd}^{\text{II}}$  transition-metal salt in a 2:2:1 molar ratio in the presence of a mild base ( $\text{Na}_2\text{CO}_3$ ) in  $\text{MeOH}/\text{CH}_2\text{Cl}_2$  (1:1 v/v) at room temperature (Figure 2).<sup>[13]</sup> Perspective views of the crystal structures of complexes **8** and **10** with atom labeling are shown in Figure 2.<sup>[12]</sup> The coordination geometry of the  $\text{Zn}^{\text{II}}$  and  $\text{Ni}^{\text{II}}$  centers in **8** and **10**, respectively, is a distorted octahedron, and the dihedral angle between the mean planes defined by O1–N1–N2–N3 and O3–N4–N5–N6 is  $93.6^\circ$  in **8** and  $92.6^\circ$  in **10**.

### Synthesis and Characterization of Neutral Metallosupramolecular Polymers

After the formation of neutral model complex **1** was achieved by subunit self-assembly, nine neutral metallosupramolecular polymers **P1–P9**, connected through neutral coordination centers, were obtained, by following the same procedure, by one-pot reaction of bisacyl hydrazide **BH1** or **BH2** with carboxaldehyde Py2al, Py2alC<sub>10</sub>, or Qui2al and a  $\text{Co}^{\text{II}}$ ,  $\text{Ni}^{\text{II}}$ ,  $\text{Zn}^{\text{II}}$ , or  $\text{Cd}^{\text{II}}$  transition-metal salt in a 1:2:1 molar ratio in the presence of a mild base ( $\text{Na}_2\text{CO}_3$ ) in  $\text{MeOH}/\text{CH}_2\text{Cl}_2$  (1:1 v/v) at room temperature (Scheme 3). The generation of **P1–P9** resulted from a self-assembly polymerization involving three processes: 1) subunit condensation to

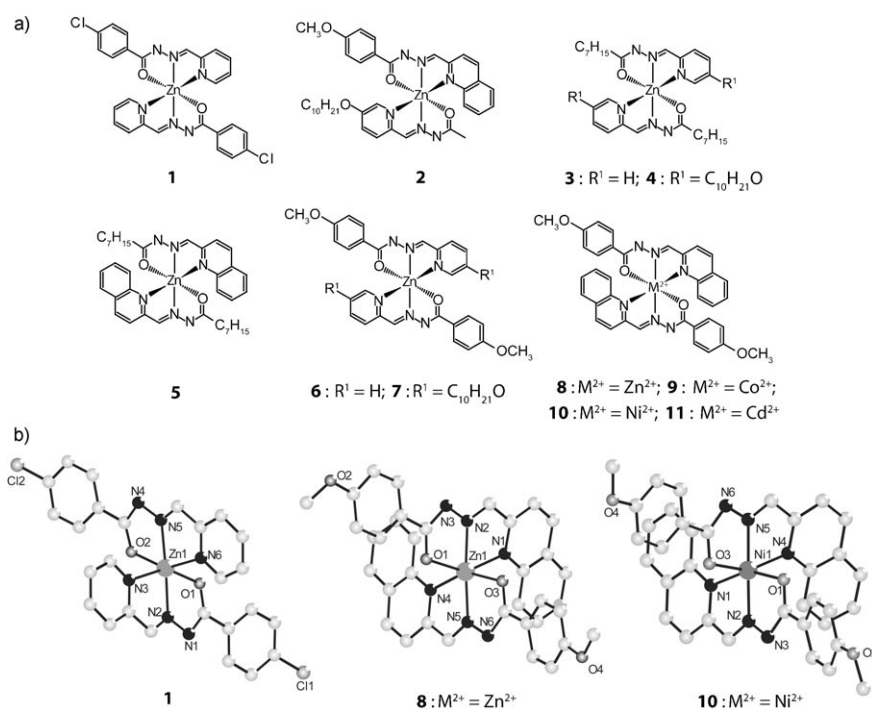


Figure 2. a) Structures of the neutral homoligand complexes **1** and **3–11** and the neutral heteroligand complex **2**. b) Perspective views of the solid-state X-ray molecular structures of complexes **1**, **8**, and **10**. Selected bond lengths for **1** (Å): Zn1–N2 2.064(3), Zn1–N3 2.306(3), Zn1–O1 2.102(3), Zn1–N5 2.060(2), Zn1–N6 2.252(2), Zn1–O2 2.095(2), N1–N2 1.367(4), N4–N5 1.365(3). The dihedral angle between the mean planes defined by O1–N1–N2–N3 and O2–N4–N5–N6 is 94.2°. Selected bond lengths for **8** (Å): Zn1–N1 2.318(3), Zn1–N2 2.065(2), Zn1–O1 2.159(2), Zn1–N4 2.238(3), Zn1–N5 2.049 (2), Zn1–O3 2.145(3), N2–N3 1.366(3), N5–N6 1.361(3). The dihedral angle between the mean planes defined by O1–N1–N2–N3 and O3–N4–N5–N6 is 93.6°. Selected bond lengths for **10** (Å): Ni1–N1 2.167(6), Ni1–N2 1.972(5), Ni1–O1 2.085(6), Ni1–N4 2.176(6), Ni1–N5 1.990(6), Ni1–O3 2.081(5), N2–N3 1.378(7), N5–N6 1.373(7). The dihedral angle between the mean planes defined by O1–N1–N2–N3 and O3–N4–N5–N6 is 92.6°.

form the tridentate coordination moiety; 2) multiple metal-ligand coordination to connect the ligand monomers; and 3) simultaneous deprotonation to form neutral coordination centers.

Different morphologies of the metallosupramolecular polymers were obtained by using different combinations of ligands and metal ions. Among the metallosupramolecular polymers, **P1** and **P3–P9** formed transparent free-standing films, whereas **P2** formed a gum after evaporation of a solution in  $\text{CH}_2\text{Cl}_2$  (Figure 3). For comparison, the free ligands **L1–L6** (Scheme 2) incorporated in the polymers were prepared independently as oily materials. The corresponding neutral model complexes **3–11** were obtained as opaque solids. All the polymers are well-soluble in common organic solvents such as  $\text{CH}_2\text{Cl}_2$ ,  $\text{CHCl}_3$ , THF, and DMF, but not in water, as the polymeric dimethylsiloxane spacer was expected to offer sufficient solubility.

$^1\text{H}$  NMR spectroscopy confirmed the formation of the supramolecular polymers. As shown in Table 1, the  $^1\text{H}$  NMR signals of the coordinated imine protons in **P1–P6** and **P9** were found at 0.33–0.85 ppm downfield of the corresponding signals of the noncoordinated imine protons in free ligands **L1–L6**. The corresponding proton signals for **P1–P9** were exactly the same as those for the neutral model complexes

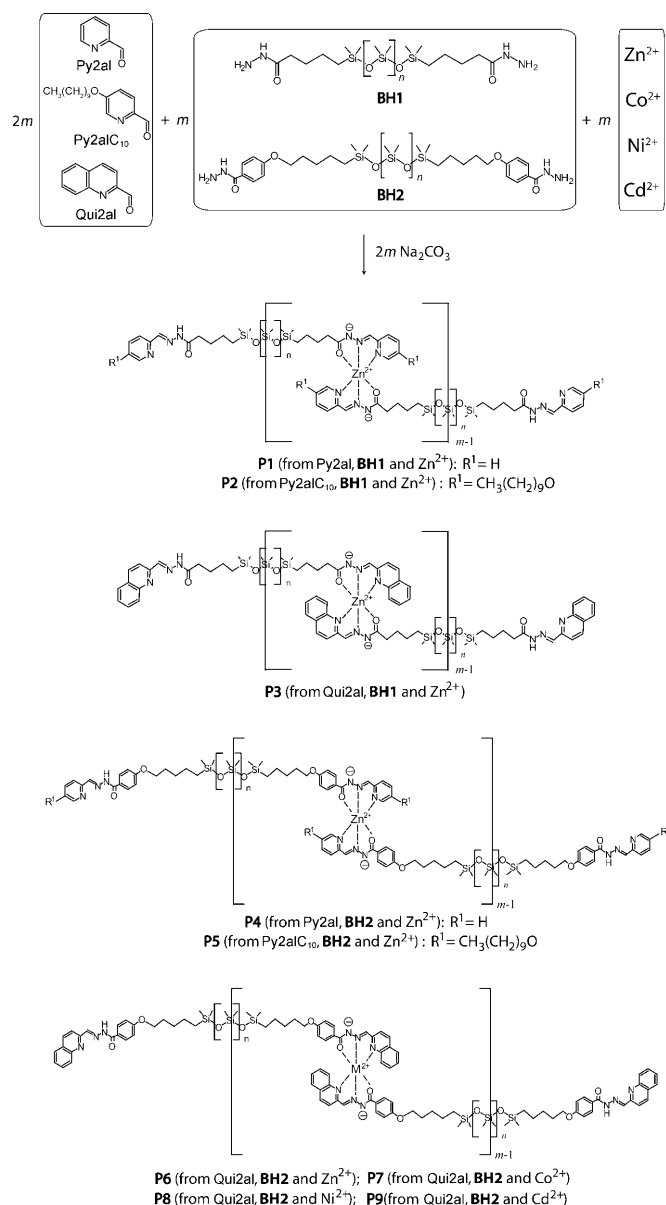
**3–11**.<sup>[13]</sup> As expected, the  $^1\text{H}$  NMR spectroscopic features of **P7** and **P8** showed that they were paramagnetic owing to the cobalt(II)  $d^7$  and nickel(II)  $d^8$  centers. The linear chain structure of the supramolecular polymers agrees with the occurrence of signals of uncomplexed terminal acyl hydrazone moieties in the  $^1\text{H}$  NMR spectra. However, the formation of large macrocyclic complexes cannot be excluded. Integration of the  $^1\text{H}$  NMR signals of the imine CH or  $\text{OCH}_2$  protons at uncomplexed and complexed coordination sites gives the average molecular weight of the metallosupramolecular polymers. As shown in Table 1, the average molecular weight of the different polymers lie in the range 33 000–52 000  $\text{g mol}^{-1}$ , which corresponds to 17–30 repeating units.  $^1\text{H}$  NMR spectroscopy also revealed the dynamic behavior of these metallosupramolecular polymers. By progressively increasing the concentration of **P1** from 3.125 through 12.5 to 50 mM in  $\text{CDCl}_3$ , its average molecular weight increased

from 15 000 through 25 000 to 41 000  $\text{g mol}^{-1}$ . The relationship between the degree of polymerization (DP), the concentration of the dissolved polymer ( $[\text{M}]$ ), and the binding constant ( $K$ ) is expressed by Equation (1).<sup>[14]</sup> Figure 4 illustrates the linear relationship between  $(\text{DP})^2$  and the concentration of **P1** dissolved in  $\text{CDCl}_3$ .

$$\text{DP} \approx (K[\text{M}])^{1/2} \quad (1)$$

Polymer **P3** presented an emission at 499 nm under excitation at 452 nm, due to the zinc(II) coordination center, which contains quinoline residues. An increase in the extension of  $\pi$  conjugation with the presence of aromatic acyl hydrazone moieties in zinc(II)-based polymers **P4–P6** led to a stronger corresponding emission at 519, 461, and 519 nm, respectively. Polymer **P9** presented an emission at 525 nm under excitation at 481 nm, due to the cadmium(II) coordination center, which contains aromatic acyl hydrazone quinoline residues. On the other hand, **P1** and **P2** were only weakly fluorescent at 450 nm under excitation at 390 nm as they only contain pyridine groups, whereas **P7** and **P8** were nonluminescent, probably due to quenching of the emission by cobalt(II) and nickel(II) ion (Table 1).





Scheme 3. Synthetic scheme of the self-assembly of metallocupramolecular polymers **P1–P9** by multiple condensation–coordination–deprotonation reactions between bis(hydrazide) **BH1** or **BH2** (0.15 mmol), aldehyde Py2al, Py2alC<sub>10</sub>, or Qui2al (0.3 mmol), and  $\text{Co}^{\text{II}}$ ,  $\text{Ni}^{\text{II}}$ ,  $\text{Zn}^{\text{II}}$ , or  $\text{Cd}^{\text{II}}$  metal salt in the presence of  $\text{Na}_2\text{CO}_3$  (0.33 mmol) in  $\text{MeOH}/\text{CH}_2\text{Cl}_2$  (1:1 v/v, 15.0 mL) at room temperature.  $n \approx 13$  for **BH1** and **BH2**.

### Selection of Combinatorial Monomeric Subunits in Ligand Self-Assembly

The use of subunits (carboxaldehyde, bis(hydrazide), and metal-ion salt) rather than presynthesized ligands (**L1–L6**) for the formation of the metallocupramolecular polymers gives an opportunity to investigate the selection of combinatorial monomeric subunits. The formation of the neutral metallocupramolecular polymer **P1** may be expected to involve  $\text{Zn}^{\text{II}}$ -mediated selection of Py2al from a library of carboxaldehydes, on the basis of its ability to form a tridentate hydrazone ligand (Scheme 4). Figure 5a shows the  $^1\text{H}$  NMR

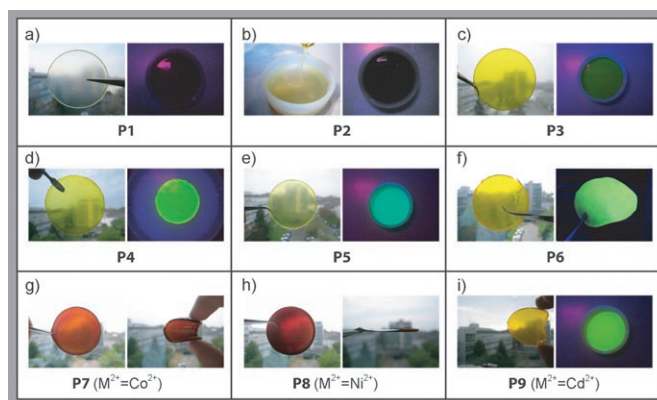


Figure 3. Photographs of samples of neutral metallocupramolecular polymers. Zinc(II)-based polymers: a) soft transparent film **P1** with weak fluorescence; b) polymer gum **P2** with weak fluorescence; c) strong transparent film **P3** with yellow fluorescence; d) strong transparent film **P4** with strong yellow fluorescence; e) soft transparent film **P5** with yellowish-green fluorescence; and f) strong transparent film **P6** with strong yellow fluorescence. Various transition-metal-based polymers: g) cobalt(II)-based polymer **P7** as a paramagnetic strong film; h) nickel(II)-based polymer **P8** as a paramagnetic strong film; and i) cadmium(II)-based polymer **P9** as a strong film with strong yellow fluorescence. The photographs of polymer fluorescence were taken under excitation at 365 nm.

spectrum of a mixture of several carboxaldehydes (Py2al, benzaldehyde, 3-chloro-4-pyridinecarboxaldehyde, 2-methoxy-3-pyridinecarboxaldehyde) and the bisacyl hydrazide monomer **BH1** in the absence of metal salt: a mixture of condensation products was obtained in different amounts (acyl hydrazone (%) / remaining aldehyde (%)) = 30:70 (benzaldehyde), 28:72 (Py2al), 35:65 (2-methoxy-3-pyridinecarboxaldehyde), 7:93 (3-chloro-4-pyridinecarboxaldehyde)). In sharp contrast, when the reaction was performed in the presence of  $\text{Zn}(\text{SO}_4) \cdot 7\text{H}_2\text{O}$ , the  $^1\text{H}$  NMR spectrum revealed that only Py2al reacted with **BH1** under coordination to the zinc(II) ions to form the corresponding polymer **P1** (Figure 5b). There was no acyl hydrazone product formed with the other three aldehydes, and all the Py2al were used up in the reaction; the new  $^1\text{H}$  NMR peaks corresponded with those of pure homopolymer **P1** (Figure 5c). The preferential formation of **P1** thus amounts to subunit selection under coordination pressure, as in the case of the generation of a grid-type metallocupramolecular architecture.<sup>[8]</sup>

### Constitutional Dynamic Behavior of Metallocupramolecular Polymers

The constitutional dynamic behavior of the present neutral metallocupramolecular polymers was demonstrated by the occurrence of cross-over ligand exchange due to the reversibility of the coordination bonds (Scheme 5), as shown by  $^1\text{H}$  NMR spectroscopic studies of polymer blends. Polymer blend **B1** was prepared by simply stacking on the top of each other two neat films of the homopolymers **P2** and **P6** in a 1:1 molar ratio at 50 °C for 24 h (without solvent or catalyst).  $^1\text{H}$  NMR spectroscopic analysis of **B1** in  $\text{CDCl}_3$

Table 1.  $^1\text{H}$  NMR chemical shifts, molecular weights, and optical properties for the metallosupramolecular polymers **P1**–**P9** depicted in Scheme 1.

Polymer	$\delta(\text{H}_{\text{imine}})$ [ppm]	$\delta(\text{H}_{\text{imine,L}})$ [ppm]	Average $M_r$ [g mol $^{-1}$ ] <sup>[b]</sup>	DP <sup>[d]</sup>	$\lambda_{\text{max,abs}}$ [nm] ( $\epsilon_{\text{max}}$ [dm $^3$ mol $^{-1}$ cm $^{-1}$ ]) <sup>[e]</sup>	$\lambda_{\text{max,ex}}$ [nm] <sup>[f]</sup>	$\lambda_{\text{max,em}}$ [nm] <sup>[f]</sup>
<b>P1</b>	8.31	7.98 ( <b>L1</b> )	33 000	20	291 (33 640), 364 (15 000)	400	456
<b>P2</b>	8.27	7.88 ( <b>L2</b> )	39 000	20	299 (27 245), 364 (26 650)	392	451
<b>P3</b>	8.61	8.14 ( <b>L3</b> )	43 000	25	274 (27 110), 304 (27 400), 400 (25 960)	452	499
<b>P4</b>	8.49	8.06 ( <b>L4</b> )	55 000	30	307 (18 330), 338 (17 905), 383 (24 375)	462	519
<b>P5</b>	8.43	8.23 ( <b>L5</b> )	38 000	17	277 (42 870), 330 (38 020), 342 (34 920), 368 (20 880)	378	461
<b>P6</b>	8.80	8.46 ( <b>L6</b> )	45 000	23	286 (31 290), 303 (31 540), 426 (34 675)	478	510
<b>P7</b>	— <sup>[a]</sup>	8.46 ( <b>L6</b> )	— <sup>[c]</sup>	— <sup>[c]</sup>	286 (35 730), 311 (40 055), 423 (58 715)	— <sup>[g]</sup>	— <sup>[g]</sup>
<b>P8</b>	— <sup>[a]</sup>	8.46 ( <b>L6</b> )	— <sup>[c]</sup>	— <sup>[c]</sup>	287 (31 370), 314 (41 350), 437 (53 855), 896 (42)	— <sup>[g]</sup>	— <sup>[g]</sup>
<b>P9</b>	8.79	8.46 ( <b>L6</b> )	52 000	26	288 (29 345), 311 (30 845), 431 (42 240)	481	525

[a] Paramagnetic materials. [b] Average molecular weight was determined by the integration of the  $^1\text{H}$  NMR signals for imine CH or  $\text{OCH}_2$  protons at uncomplexed and complexed coordination sites of each polymer at 25 mm in  $\text{CDCl}_3$ . [c] Paramagnetic materials; could not determined by integration of  $^1\text{H}$  NMR signals. [d] Degree of polymerization = number of repeating units in polymer chain. [e] Electronic spectroscopic measurements were obtained in  $\text{CHCl}_3$  at 298 K. [f] Spectrofluorimetric measurements were performed at 0.20 mm in  $\text{CHCl}_3$ . [g] Non-emissive materials.

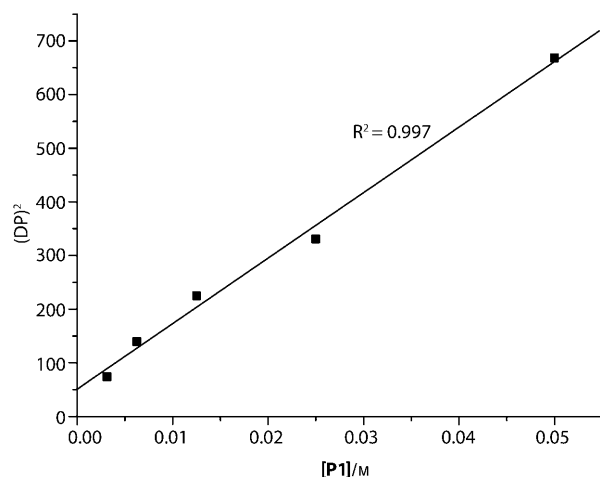


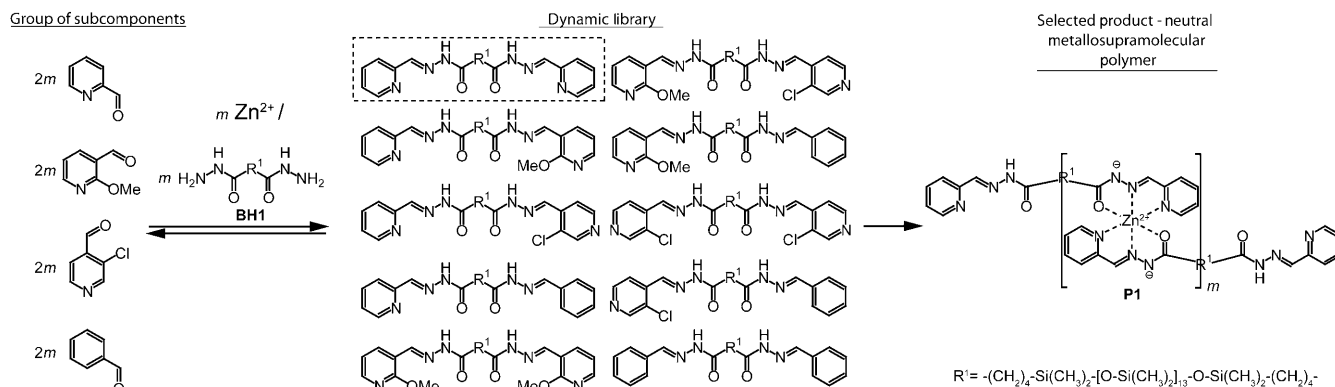
Figure 4. Relationship between DP and the concentration of **P1** in  $\text{CDCl}_3$  according to Equation (1). The slope and vertical intercept of the best-fit  $(\text{DP})^2$  versus  $[\text{P1}]$  plot are  $(1.22 \pm 0.054) \times 10^4 \text{ M}^{-1}$  and  $5.10 \pm 0.042 \times 10^2$ , respectively.

( $\approx 50$  mm) allowed identification of the various types of connections between zinc ion and acyl hydrazone ligands by the signals of the C–H protons of the imine and aromatic

groups between 6.6–8.9 ppm (Figure 6). The spectrum of **B1** showed three characteristic imine proton signals, which were assigned to 1) **P2** (8.27 ppm): starting homopolymer; 2) **P6** (8.80 ppm): starting homopolymer; and, most importantly, 3) a new imine peak (8.60 ppm): a new heteroligand zinc(II) coordination polymer containing both **L2** and **L6**. Confirmation was obtained by synthesizing monomeric  $\text{Zn}^{\text{II}}$  complex **2** as a reference compound. These results indicate that the blending of two different metallodynamers generated a new heteroligand metallosupramolecular polymer by ligand exchange (even in the neat phase without catalyst). The random copolymer **C1** was also prepared as a reference material by reaction of a mixture of the free ligands **L2** and **L6** with  $\text{Zn}^{\text{II}}$  metal salt in a 1:1:2 molar ratio. The  $^1\text{H}$  NMR signals found for **C1** were exactly the same as those for **B1** (Figure 6e). Integration of the  $^1\text{H}$  NMR signals for the  $\text{CH}_2$  (C=O) and CH(imine) protons of uncomplexed and complexed

coordination sites gave an average molecular weight of around  $28000 \text{ g mol}^{-1}$ , which is of the same order as the parent polymers **P2** and **P6**. On the basis of the appearance of the uncomplexed coordination sites as end groups, linear coordination polymer structures can be inferred. To study the kinetics of the dynamic ligand-exchange reaction between homopolymers **P2** and **P6**,  $^1\text{H}$  NMR spectroscopic analysis was performed on 1:1 mixtures of **P2** and **P6** (2.5 mm each) at 25 °C in  $\text{CDCl}_3$ ; however, equilibrium was reached as soon as **P2** and **P6** were mixed.

The degree of constitutional dynamic evolution was correlated with the ratio of **P2** and **P6** incorporated in the polymer blend. Polymer blends **B2** and **B3** were prepared in the same way as **B1** except that when stacking the homopolymers **P2** and **P6**, the molar ratio 1:1 was replaced by 2:1 (**B2**) and 1:2 (**B3**). As expected, the  $^1\text{H}$  NMR spectra of **B1**–**B3** showed the three characteristic imine proton signals (Figure 7). The ratio of the areas of the signals assigned to the **P2/P6** heteroligand polymer was found to be about 1:1:2 in **B1**, as opposed to 6:1:4 and 1:6:4 in **B2** and **B3**, respectively. These results indicate that the outcome of the constitutional dynamic behavior can be statistically correlated with the ratio of **P2** and **P6** used in the polymer blend.



Scheme 4. Preferential formation of the neutral metallosupramolecular polymer **P1** through Zn<sup>II</sup>-mediated selection of Py2al from a library of carboxaldehydes based on the ability to form a bistridentate acyl hydrazone ligand (highlighted).

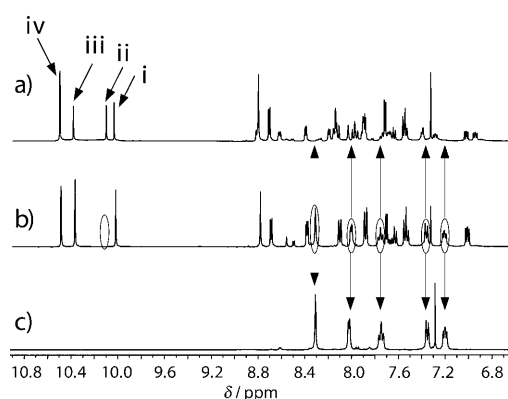


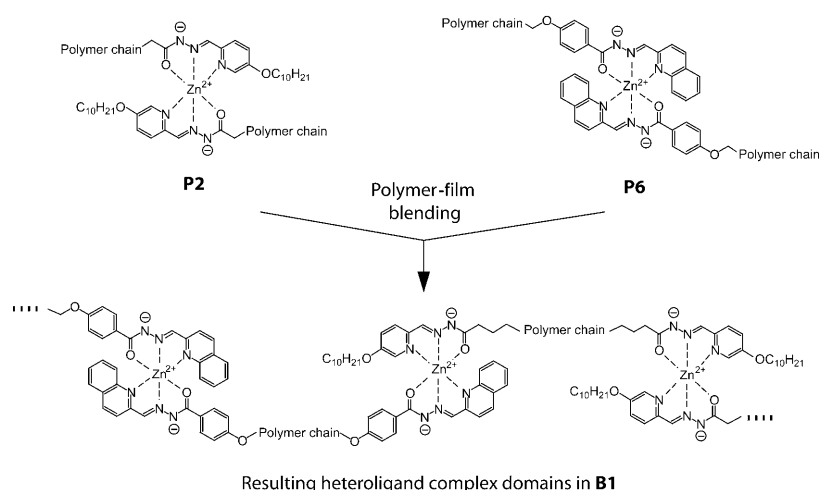
Figure 5.  $^1\text{H}$  NMR spectra of the condensation reaction between a mixture of carboxaldehydes (i = benzaldehyde, ii = pyridine-2-carboxaldehyde, iii = 2-methoxy-3-pyridinecarboxaldehyde, iv = 3-chloro-4-pyridinecarboxaldehyde) and bishydrazide monomer **BH1** (2:2:2:2:1 ratio) in the a) absence and b) presence of  $\text{Zn}(\text{SO}_4) \cdot 7\text{H}_2\text{O}$ . c)  $^1\text{H}$  NMR spectrum of homopolymer **P1** (control). The signals highlighted in b) show the disappearance of ii and the appearance of **P1**.

# Transformation of Mechanical and Optical Properties by Dynamic Constitutional Exchange in Metallosupramolecular Polymers

Materials may introduce new functional properties through dynamic constitutional metal–ligand exchange in dynamers. For example, optical properties can be easily transformed through component incorporation. Polymer blends **B4–B6** were prepared by stacking 33, 50, and 67 mol % of **P8** with respect to **P2**, respectively, at 50 °C for 24 h in the absence of solvent. **P2**, which contains two acyl hydrazone–pyridine units, is a very weakly emissive gum, whereas **P8** is a non-emissive film because of the presence of the paramagnetic Ni<sup>II</sup> metal center. Spectrofluorimetric analysis of the exchanged polymer blends **B4–B6** in CHCl<sub>3</sub> allowed identification of the dynamic exchange between metal ions and acyl hydrazone ligands by following their optical properties (Figure 8a). **B4–B6** all showed an excitation maximum at 478 nm and an emission maximum at 512 nm, which were fully matched to the excitation and emission spectra of homopolymer **P6** (one of the main luminescent domains in the

polymer blends). This indicates that cross-over metal-cation exchange had occurred during the preparation of the film of the polymer blend. Figure 8b shows the optical features of **P2**, **P8**, **B5** (before exchange reaction) and **B5** (after exchange).

Evolution of the mechanical properties<sup>[5h]</sup> of **B4–B6** was also observed. **P2**, which contains two decyloxy pyridine units, is a gum, whereas **P8** is a hard film because of the presence of aromatic-type acyl hydrazone and quinoline moieties. Viscoelasticity measurements revealed that the storage elastic modulus  $E'$  of **P8** was  $8.33 \times 10^{-2}$  GPa at 25 °C, and the profile of the loss



Scheme 5. Constitutional metal–ligand exchange reaction between metallodynamers **P2** and **P6**: evolution of metallodynamers that contain only homoligand domains into polymer blend **B1**, which contains heteroligand domains.



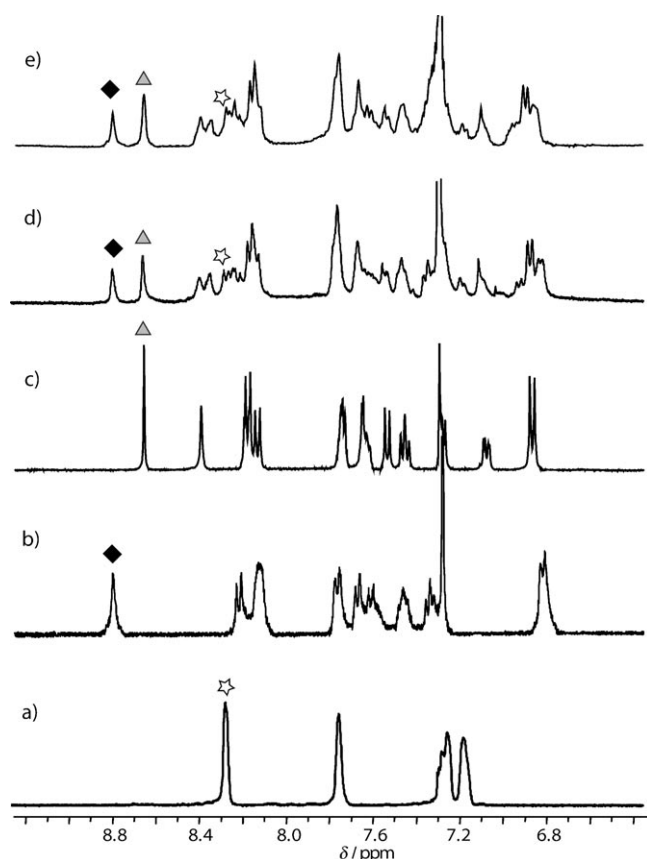


Figure 6. Section of the  $^1\text{H}$  NMR spectra of a) polymer **P2**, b) polymer **P6**, c) reference heteroligand complex **2**, d) blend **B1**, and e) copolymer **C1** in  $\text{CDCl}_3$  ( $\approx 50$  mm), showing the C–H proton signals of the imine or aromatic entities. The symbols indicate the corresponding characteristic proton signals in the spectra (star = **P2**, diamond = **P6**) and the new heteroligand polymer (triangle).

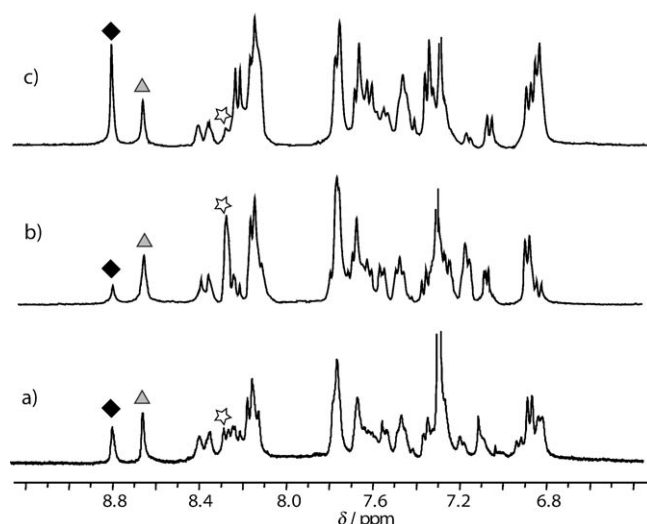


Figure 7. Section of the  $^1\text{H}$  NMR spectra of the blended polymers a) **B1** (from **P2/P6** = 1:1), b) **B2** (from **P2/P6** = 2:1), and c) **B3** (from **P2/P6** = 1:2) in  $\text{CDCl}_3$  ( $\approx 50$  mm). The symbols indicate the corresponding characteristic proton signals of the reference polymers (star = **P2**, diamond = **P6**) and the new heteroligand polymer (triangle).

elastic modulus,  $E''$ , gave the  $T_m$  value of **P8** as  $83.5^\circ\text{C}$  (Table 2). These results are in line with the gum and hard-film behavior of **P2** and **P8**, respectively (Figure 8). As the polymer blends **B4–B6** are composed of 33, 50, and 66 mol % of **P8** (hard segment) with respect to **P2**, respectively, the increase in  $E'$  and  $T_m$  values from **B4** to **B6** correlates with the molar percentage of **P8** present (Table 2). This correlation is nicely reflected in the difference in film hardness at room temperature among **B4–B6** (Figure 8d). Scheme 6 shows the proposed constitutional metal–ligand exchange reaction between metallodynamers **P2** and **P8**.

## Conclusions

The present results demonstrate that neutral metallosupramolecular polymers can be rationally designed and synthesized in a selective, self-assembly manner. They also reveal that these coordination polymers are indeed dynamic, capable of interchanging the elements (ligand components and metal ions) of their coordination centers in solution as well as in the neat phase, thus allowing the introduction of novel properties, a particularly attractive feature of such functional dynamic materials. At the meeting point of metallosupramolecular chemistry, coordination chemistry, and polymer chemistry, coordination polymers are constitutional dynamic materials, or metallodynamers, that offer a rich palette of entities and properties resulting from the blending of constitutional dynamic chemistry with pure and applied materials science.

## Experimental Section

### General

Pyridine-2-carboxaldehyde, 2-quinoline-carboxaldehyde, benzaldehyde, 2-methoxy-3-pyridinecarboxaldehyde, 3-chloro-4-pyridinecarboxaldehyde,  $\text{Co}(\text{BF}_4)_2 \cdot 6\text{H}_2\text{O}$ ,  $\text{Ni}(\text{BF}_4)_2 \cdot 6\text{H}_2\text{O}$ ,  $\text{Zn}(\text{SO}_4) \cdot 7\text{H}_2\text{O}$ ,  $\text{Cd}(\text{NO}_3)_2 \cdot 4\text{H}_2\text{O}$ , octyloic hydrazide, 4-methoxybenzhydrazide, 1-iododecane, ethyl-4-pentenoate, hydrazine monohydrate, 4-hydroxymethylbenzoate, and 5-bromo-1-pentene were obtained from Aldrich. Hydrogen-terminated polydimethylsiloxane ( $M_n \approx 1000\text{--}1100$   $\text{g mol}^{-1}$ ) and Karstedt catalyst were obtained from ABCN. 5-Hydroxypyridine-2-carboxaldehyde was prepared according to the literature method.<sup>[15]</sup> Deuterated chloroform used for the kinetic measurements was flushed through basic alumina immediately prior to use to remove any trace of acid.  $^1\text{H}$  NMR spectra were recorded on a Bruker 400-MHz Ultrashield Avance 400 spectrometer. UV/Vis spectra were recorded on a Varian-Cary-3 spectrometer or on a Jasco V-560 spectrometer. EI and ES MS was performed by the Service de Spectrométrie de Masse, Université Louis Pasteur. Elementary analysis was performed on a Vario EL elementary analyzer. Details about data collection and solution refinement are given in the Supporting Information. X-ray diffraction measurements for complex **1** were performed on a Nonius Kappa CCD diffractometer operating with an  $\text{MoK}\alpha$  ( $\lambda = 0.71073$  Å) X-ray tube with a graphite monochromator. The structure was solved (SHELXS-97) by direct methods and refined (SHELXL-97) by full-matrix least-square procedures on  $F^2$ . All non-H atoms were refined anisotropically.<sup>[12]</sup>

### Syntheses

**E2**: A mixture of 4-hydroxymethylbenzoate (5.45 g, 35.8 mmol), 5-bromo-1-pentene (4.85 g, 32.5 mmol),  $\text{K}_2\text{CO}_3$  (22 g, 163 mmol), KI

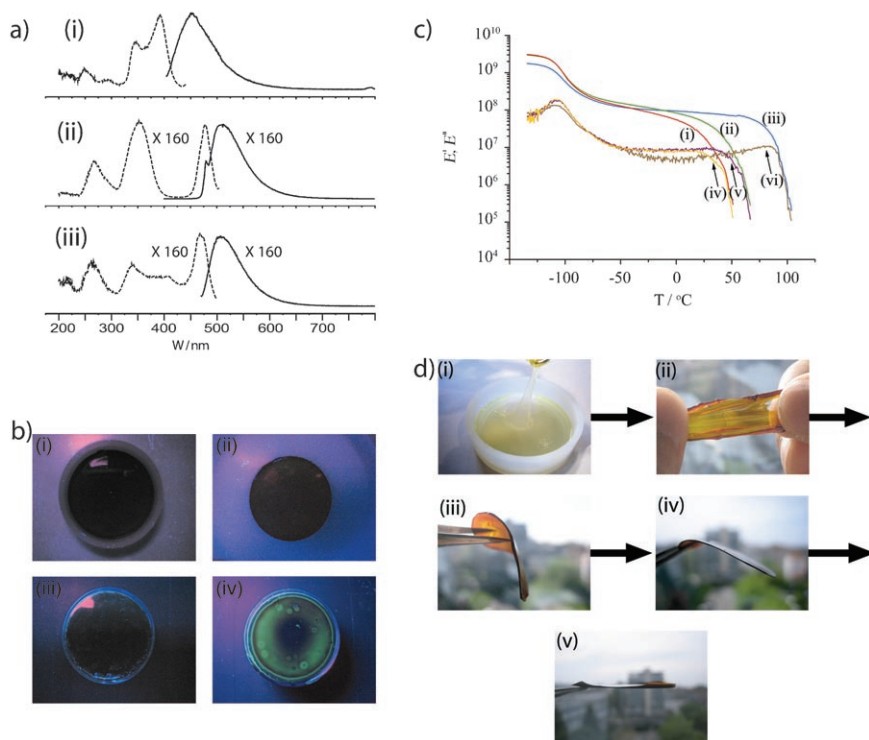


Figure 8. Evolution of the optical properties of the metallodynamers. a) Excitation (dashed line) and emission (solid line) spectra of i) **P2**, ii) **P6**, and iii) polymer blend **B5** in  $\text{CHCl}_3$  (0.2 mm). b) Photographs of the metallodynamer films taken under excitation at 365 nm: nonfluorescent films i) **P2**, ii) **P8**, and iii) **B5** before the exchange reaction, and iv) fluorescent film **B5** after exchange. c) Temperature dependence of the storage elastic modulus  $E'$  of the films i) blend **B5**, ii) blend **B6**, and iii) **P8**, and of the loss elastic modulus  $E''$  of the films iv) blend **B5**, v) blend **B6**, and vi) **P8**. d) Visualization of the progressive soft-to-hard evolution of the mechanical properties of the metallodynamers i) **P2** (gum), ii) blend **B4** (very soft and stretchy material), iii) blend **B5** (soft film), iv) blend **B6** (hard film), and v) **P8** (hard film).

Table 2. Evolution in mechanical properties of the dynamic metallodipramolecular polymers **P2**, **P8**, **B4**, **B5**, and **B6** as a function of the amount of incorporation of **P8** into **P2**.

Polymer	<b>P8/P2</b> [mol %]	$T_m$ [°C] <sup>[a]</sup>	$E'$ [GPa] <sup>[b]</sup>
<b>P2</b>	0	−32.3 <sup>[c]</sup>	— <sup>[d]</sup>
<b>B4</b>	33	−20.1 <sup>[c]</sup>	— <sup>[d]</sup>
<b>B5</b>	50	19.1	$8.35 \times 10^{-3}$
<b>B6</b>	67	33.5	$9.77 \times 10^{-3}$
<b>P8</b>	100	83.5	$1.08 \times 10^{-2}$

[a] Melting temperature determined by the profile of the loss elastic modulus  $E''$ . [b] Storage elastic modulus  $E'$  at the melting temperature. [c] Melting temperature determined by differential scanning calorimetry. [d] Materials were a gum.

(0.55 g, 3.25 mmol), and acetone (200 mL) was heated at reflux with stirring under nitrogen overnight. The white solid in the reaction mixture was filtered out. The filtrate collected was concentrated by using a rotary evaporator. A crude yellow oil was obtained. TLC analysis of the crude product (heptane/diethyl ether=4:1) gave  $R_f$ =0 (starting material) and 0.5 (product). The crude oil was purified by silica-gel column chromatography to give 4-(pent-4-en-1-yn-1-yl)methylbenzoate (**E2**; 85%) as a colorless oil.  $^1\text{H}$  NMR ( $\text{CDCl}_3$ ):  $\delta$ =8.00 (d,  $J$ =8.97 Hz, 2H), 6.92 (d,  $J$ =8.94 Hz, 2H), 5.92–5.81 (m, 1H), 5.11–5.01 (m, 2H), 4.04 (t,  $J$ =6.43 Hz, 2H), 3.90 (s, 3H), 2.26 (q,  $J$ =6.89 Hz, 2H), 1.92 ppm (quint,  $J$ =6.82 Hz, 2H); MS (ESI+):  $m/z$ =221 [ $M+H$ ]<sup>+</sup>; elemental analysis: calcd (%) for  $\text{C}_{13}\text{H}_{16}\text{O}_3$ : C 70.89, H 7.32; found: C 71.06, H 7.32.

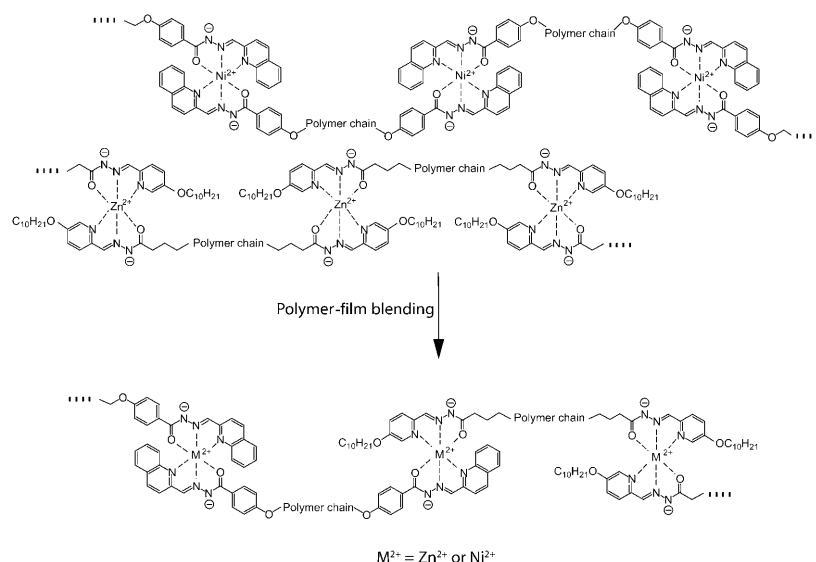
**Py2alC<sub>10</sub>**: A mixture of 5-hydroxypyridine-2-carboxyaldehyde<sup>[15]</sup> (0.414 g, 3.64 mmol), 1-iododecane (1.35 g, 5.1 mmol),  $\text{K}_2\text{CO}_3$  (1.25 g, 9.1 mmol), and anhydrous DMF (40 mL) was heated to 80°C with stirring under nitrogen overnight. The white solids in the reaction mixture were then filtered out. The filtrate collected was concentrated by using a rotary evaporator. TLC analysis of the crude product (petroleum ether/ethyl acetate=7.5:1) gave  $R_f$ =0 (unknown side product) and 0.5 (product). The crude solid was purified by silica-gel column chromatography to give **Py2alC<sub>10</sub>** (90%) as a white crystalline solid.  $^1\text{H}$  NMR ( $\text{CDCl}_3$ ):  $\delta$ =10.00 (s, 1H), 8.44 (d,  $J$ =2.68 Hz, 1H), 7.97 (d,  $J$ =8.65 Hz, 1H), 7.30 (dd,  $J$ =8.67, 2.99 Hz, 1H), 4.11 (t,  $J$ =6.52 Hz, 2H), 1.91–1.81 (m, 2H), 1.54–1.43 (m, 2H), 1.43–1.22 (m, 12H), 0.90 ppm (t,  $J$ =6.84 Hz, 3H); MS (ESI+):  $m/z$ =264 [ $M+H$ ]<sup>+</sup>; elemental analysis: calcd (%) for  $\text{C}_{16}\text{H}_{25}\text{NO}_3$ : C 72.96, H 9.57, N 5.32; found: C 72.77, H 9.67, N 5.24.

**BE1**: Ethyl-4-pentenoate (**E1**; 3.1 g, 24 mmol) was added to hydrogen-terminated toluene polydimethylsiloxane (50 mL, 11 g, 10 mmol). Karstedt catalyst (platinum divinyltetramethyldisiloxane complex in xylene, 4 drops) was then added to the mixture. The reaction mixture was stirred at room temperature under nitrogen overnight. During the course of the reaction, the solution turned from colorless to pale yellow. The reaction was exothermic during the first 10 min. Silica gel was

used to remove the Karstedt catalyst by simply loading the resulting mixture in toluene on a column and eluting with  $\text{CH}_2\text{Cl}_2$  (250 mL). The elutant was concentrated to give polydimethylsiloxanes- $\alpha,\omega$ -bis(ethyl-1-pentanoate) (**BE1**; 98%) as a colorless oil, which was used without further purification. As a result of the molecular-weight dispersion of the product, characterization was based mainly on NMR spectroscopy.  $^1\text{H}$  NMR ( $\text{CDCl}_3$ ):  $\delta$ =4.13 (q,  $J$ =7.13 Hz, 4H), 2.30 (t,  $J$ =7.54 Hz, 4H), 1.66 (quint,  $J$ =7.50 Hz, 4H), 1.43–1.33 (m, 4H), 1.26 (t,  $J$ =7.14 Hz, 6H), 0.56 (t,  $J$ =7.60 Hz, 4H), 0.09 ppm (s, 90H).

**BE2**: The same procedure as that used for **BE1** was used to synthesize polydimethylsiloxanes- $\alpha,\omega$ -bis[4-(pentan-4-oxo)methylbenzoate] (**BE2**; 98%) by replacing **E1** with **E2**. The colorless oil obtained was used without further purification. As a result of the molecular-weight dispersion of the product, characterization was based mainly on NMR spectroscopy.  $^1\text{H}$  NMR ( $\text{CDCl}_3$ ):  $\delta$ =8.00 (d,  $J$ =8.91 Hz, 4H), 6.92 (d,  $J$ =8.89 Hz, 4H), 4.03 (t,  $J$ =6.54 Hz, 4H), 3.91 (s, 6H), 1.83 (quint,  $J$ =6.65 Hz, 4H), 1.57–1.47 (m, 4H), 1.47–1.37 (m, 4H), 0.60 (t,  $J$ =7.67 Hz, 4H), 0.10 ppm (s, 90H).

**BH1**: A solution of **BE1** (12.6 g, 10.0 mmol) in ethanol (15 mL) was added to hydrazine monohydrate (10 g, 200 mmol). The reaction mixture was heated at reflux and stirred under nitrogen for 24 h. The reaction mixture was concentrated. TLC analysis of the crude product with  $\text{CHCl}_3/\text{MeOH}$  (25:1) gave  $R_f$ =0.05 (hydrazine) and 0.25 (product). The crude oil was purified by silica-gel column chromatography to yield polydimethylsiloxanes- $\alpha,\omega$ -bis(pentanoic-1-hydrazide) (**BH1**; 95%) as a colorless oil. **BH1** was kept in a refrigerator. As a result of the molecular-weight dispersion of the product, characterization was based mainly on NMR spectroscopy.  $^1\text{H}$  NMR ( $\text{CDCl}_3$ ):  $\delta$ =6.85 (br, 2H), 3.21 (br, 4H),



Scheme 6. Dynamic constitutional interchange of the elements (ligand and metal ions) of the coordination centers of **P2** and **P8** to result in a new functional polymer blend, and proposed constitutional metal-ligand exchange reaction between metallodynamers **P2** and **P8**: evolution of the domains in the metal coordination complexes from two homotypes in the metallodynamers **P2** and **P8** into six different types in the polymer blends **B4–B6**.

2.18 (t,  $J=7.66$  Hz, 4H), 1.69 (quint,  $J=7.56$  Hz, 4H), 1.36–1.26 (m, 4H), 0.57 (t,  $J=8.30$  Hz, 4H), 0.09 ppm (s, 90H).

**BH2**: The same procedure as that used for the synthesis of **BH1** was used to synthesize **BH2**, with **BE1** replaced by **BE2**. TLC analysis of the crude product with  $CHCl_3/MeOH$  (5:1) gave  $R_f=0.05$  (hydrazine) and 0.8 (product). The crude oil was purified by silica-gel column chromatography to yield polydimethylsiloxanes- $\alpha,\omega$ -bis[4-(pentan-4-oxy)benzoic-1-hydrazide] (**BH2**; 95 %) as a pale-yellow oil. **BH2** was kept in a refrigerator. As a result of the molecular-weight dispersion of the product, characterization was based mainly on NMR spectroscopy.  $^1H$  NMR ( $CDCl_3$ ):  $\delta=7.72$  (d,  $J=8.69$  Hz, 4H), 6.94 (d,  $J=8.68$  Hz, 4H), 4.01 (t,  $J=6.37$  Hz, 4H), 1.83 (quint,  $J=6.52$  Hz, 4H), 1.55–1.46 (m, 4H), 1.46–1.36 (m, 4H), 0.60 (t,  $J=7.66$  Hz, 4H), 0.10 ppm (s, 90H).

**L1**: A mixture of Py2al (0.15 mmol), **BH1** (0.075 mmol), and anhydrous  $Na_2SO_4$  (1.5 mmol) was stirred at room temperature under  $N_2$  for 24 h in  $CH_2Cl_2$  (7.50 mL). The crude oil was purified by silica-gel column chromatography ( $CH_2Cl_2/MeOH=40:1$ ) to give **L1** (95 %) as a pale-yellow oil. As a result of the molecular-weight dispersion of the product, characterization was based mainly on NMR spectroscopy.  $^1H$  NMR spectrum ( $CDCl_3$ ):  $\delta=8.61$  (d,  $J=6.94$  Hz, 2H), 7.98 (s, 2H), 7.94 (d,  $J=7.98$  Hz, 2H), 7.72 (t,  $J=7.96$  Hz, 2H), 7.27 (t,  $J=6.98$  Hz, 2H), 2.78 (t,  $J=7.75$  Hz, 4H), 1.77 (quint,  $J=7.65$  Hz, 4H), 1.52–1.41 (m, 4H), 0.67–0.58 (m, 4H), 0.10 ppm (s, 90H).

**L2**: A mixture of Py2alC<sub>10</sub> (0.15 mmol), **BH1** (0.075 mmol), and anhydrous  $Na_2SO_4$  (1.5 mmol) was stirred at room temperature under  $N_2$  for 24 h in  $CH_2Cl_2$  (7.50 mL). The crude product was purified by silica-gel column chromatography ( $CH_2Cl_2/MeOH=40:1$ ) to give **L2** (89 %) as a pale-yellow oil. As a result of the molecular-weight dispersion of the product, characterization was based mainly on NMR spectroscopy.  $^1H$  NMR ( $CDCl_3$ ):  $\delta=8.28$  (d,  $J=2.88$  Hz, 2H), 7.90 (d,  $J=8.00$  Hz, 2H), 7.88 (s, 2H), 7.34 (d,  $J=8.04$  Hz, 2H), 4.06 (t,  $J=6.46$  Hz, 4H), 2.76 (t,  $J=7.66$  Hz, 4H), 1.90–1.72 (m, 8H), 1.54–1.42 (m, 8H), 1.42–1.24 (m, 24H), 0.90 (t,  $J=6.80$  Hz, 6H), 0.66–0.56 (m, 4H), 0.09 ppm (s, 90H).

**L3**: A mixture of Qui2al (0.15 mmol), **BH1** (0.075 mmol), and anhydrous  $Na_2SO_4$  (1.5 mmol) were stirred at room temperature under  $N_2$  for 24 h in  $CH_2Cl_2$  (7.50 mL). The crude product was purified by silica-gel column chromatography ( $CH_2Cl_2/MeOH=50:1$ ) to give **L3** (91 %) as a pale-yellow oil. As a result of the molecular-weight dispersion of the product,

characterization was based mainly on NMR spectroscopy.  $^1H$  NMR ( $CDCl_3$ ):  $\delta=8.17$  (d,  $J=9.15$  Hz, 2H), 8.14 (s, 2H), 8.12–8.05 (m, 4H), 7.83 (d,  $J=8.05$  Hz, 2H), 7.74 (t,  $J=7.69$  Hz, 2H), 7.57 (t,  $J=7.48$  Hz, 2H), 2.85 (t,  $J=7.63$  Hz, 4H), 1.83 (quint,  $J=7.94$  Hz, 4H), 1.51 (quint,  $J=7.88$  Hz, 4H), 0.68 (t,  $J=8.05$  Hz, 4H), 0.10 ppm (s, 90H).

**L4**: A mixture of Py2al (0.15 mmol), **BH2** (0.075 mmol), and anhydrous  $Na_2SO_4$  (1.5 mmol) was stirred at room temperature under  $N_2$  for 24 h in  $CH_2Cl_2$  (7.50 mL). The crude oil was purified by silica-gel column chromatography ( $CH_2Cl_2/MeOH=40:1$ ) to give **L4** (95 %) as a pale-yellow oil. As a result of the molecular-weight dispersion of the product, characterization was based mainly on NMR spectroscopy.  $^1H$  NMR spectrum ( $CDCl_3$ ):  $\delta=8.51$  (d,  $J=6.99$  Hz, 2H), 8.06 (s, 2H), 8.00–7.87 (m, 6H), 7.66 (t,  $J=7.85$  Hz, 2H), 7.22 (t,  $J=7.77$  Hz, 2H), 6.86 (d,  $J=7.88$  Hz, 4H), 4.04 (t,  $J=6.48$  Hz, 4H), 1.87–1.73 (m, 4H), 1.56–1.35 (m, 8H), 0.65–0.54 (m, 4H), 0.10 ppm (s, 90H).

**L5**: A mixture of Py2alC<sub>10</sub> (0.15 mmol), **BH2** (0.075 mmol), and anhydrous  $Na_2SO_4$  (1.5 mmol) was stirred at room temperature under  $N_2$  for 24 h in  $CH_2Cl_2$  (7.50 mL). The crude product was purified by silica-gel column chromatography ( $CH_2Cl_2/MeOH=60:1$ ) to give **L5** (92 %) as a pale-yellow oil. As a result of the molecular-weight dispersion of the product, characterization was based mainly on NMR spectroscopy.  $^1H$  NMR ( $CDCl_3$ ):  $\delta=8.23$  (s, 2H), 7.97 (d,  $J=8.48$  Hz, 4H), 7.44 (s, 2H), 7.34 (d,  $J=7.05$  Hz, 2H), 7.20 (d,  $J=7.04$  Hz, 2H), 6.98 (d,  $J=8.46$  Hz, 4H), 4.08 (t,  $J=6.48$  Hz, 4H), 4.02 (t,  $J=6.22$  Hz, 4H), 1.89–1.75 (m, 8H), 1.48–1.40 (m, 12H), 1.40–1.22 (m, 24H), 0.90 (t,  $J=6.53$  Hz, 6H), 0.65–0.55 (m, 4H), 0.09 ppm (s, 90H).

**L6**: A mixture of Qui2al (0.15 mmol), **BH2** (0.075 mmol), and anhydrous  $Na_2SO_4$  (1.5 mmol) were stirred at room temperature under  $N_2$  for 24 h in  $CH_2Cl_2$  (7.50 mL). The crude product was purified by silica-gel column chromatography ( $CH_2Cl_2/MeOH=50:1$ ) to give **L6** (91 %) as a pale-yellow oil. As a result of the molecular-weight dispersion of the product, characterization was based mainly on NMR spectroscopy.  $^1H$  NMR ( $CDCl_3$ ):  $\delta=8.46$  (s, 2H), 8.18 (d,  $J=8.84$  Hz, 2H), 8.12 (d,  $J=8.58$  Hz, 2H), 8.06 (d,  $J=8.49$  Hz, 2H), 7.96 (d,  $J=7.99$  Hz, 4H), 7.79 (d,  $J=7.05$  Hz, 2H), 7.69 (t,  $J=8.31$  Hz, 2H), 7.54 (t,  $J=7.01$  Hz, 2H), 6.94 (d,  $J=6.99$  Hz, 4H), 4.01 (t,  $J=6.31$  Hz, 4H), 1.82 (quint,  $J=6.67$  Hz, 4H), 1.54–1.36 (m, 8H), 0.62 (t,  $J=6.73$  Hz, 4H), 0.11 ppm (s, 90H).

**L7**: A mixture of Qui2al (6 mmol) and 4-methoxybenzhydrazide (6 mmol) was stirred and heated at reflux under  $N_2$  for 4 h in EtOH (20 mL). The solvent was removed by rotary evaporation. The crude product was purified by silica-gel column chromatography to give **L7** (91 %) as a shiny solid.  $^1H$  NMR ( $CD_3OD$ ):  $\delta=8.46$  (s, 1H), 8.18 (d,  $J=8.88$  Hz, 1H), 8.12 (d,  $J=8.78$  Hz, 1H), 8.06 (d,  $J=8.49$  Hz, 1H), 7.96 (d,  $J=7.99$  Hz, 2H), 7.79 (d,  $J=7.05$  Hz, 1H), 7.69 (t,  $J=8.31$  Hz, 1H), 7.54 (t,  $J=7.05$  Hz, 1H), 6.94 (d,  $J=6.98$  Hz, 2H), 4.01 ppm (s, 3H); MS (ESI<sup>+</sup>):  $m/z=306$  [ $M+H$ ]<sup>+</sup>; elemental analysis: calcd (%) for  $C_{18}H_{15}N_3O_2 \cdot CH_3CH_2OH$ : C 68.36, H 6.02, N 13.66; found: C 68.31, H 5.99, N 13.67.

**L8**: A mixture of Py2alC<sub>10</sub> (1 mmol) and acethydrazide (1 mmol) was stirred and heated at reflux under  $N_2$  for 4 h in EtOH (10 mL). The solvent was removed by rotary evaporation. The crude product was purified by silica-gel column chromatography to give **L8** (95 %) as a shiny white solid.  $^1H$  NMR ( $CDCl_3$ ):  $\delta=8.28$  (d,  $J=2.78$  Hz, 1H), 7.89 (d,  $J=8.80$  Hz, 1H), 7.87 (s, 1H), 7.24 (dd,  $J=2.80, 8.75$  Hz, 1H), 4.06 (t,  $J=$



6.52 Hz, 2H), 2.39 (s, 3H), 1.86–1.79 (m, 2H), 1.52–1.42 (m, 2H), 1.42–1.24 (m, 12H), 0.90 ppm (t,  $J=6.83$  Hz, 3H); MS (ESI+):  $m/z=320$  [ $M+H$ ] $^+$ ; elemental analysis: calcd (%) for  $C_{18}H_{29}N_3O_2$ : C 67.68, H 9.15, N 13.15; found: C 67.44, H 9.10, N 13.23.

General procedure for the preparation of **1** and **3–11**: The self-assembly reaction was performed by adding pyridine-2-carboxaldehyde (Py2al, Py2alC<sub>10</sub>, or Qui2al; 3 mmol), acyl hydrazide (4-chlorobenzoic hydrazide, octyloic hydrazide, or 4-methoxybenzhydrazide; 3 mmol), transition-metal salt (Co<sup>II</sup>, Ni<sup>II</sup>, Zn<sup>II</sup>, or Cd<sup>II</sup>; 1.5 mmol), Na<sub>2</sub>CO<sub>3</sub> (3.3 mmol), and anhydrous Na<sub>2</sub>SO<sub>4</sub> (30 mmol) in MeOH/CH<sub>2</sub>Cl<sub>2</sub> (1:1 v/v, 50.0 mL). The reaction mixture was stirred at room temperature under N<sub>2</sub> for 4 h. Na<sub>2</sub>CO<sub>3</sub> and Na<sub>2</sub>SO<sub>4</sub> were then filtered out. The clear solution was reduced in volume and washed with diethyl ether.

**1**: Yellow crystals were obtained by slow evaporation in EtOH/CH<sub>2</sub>Cl<sub>2</sub> (1:1 v/v). <sup>1</sup>H NMR (CDCl<sub>3</sub>):  $\delta=8.53$  (s, 2H), 8.18 (d,  $J=8.53$  Hz, 4H), 8.06 (d,  $J=7.29$  Hz, 2H), 7.77 (t,  $J=7.68$  Hz, 2H), 7.42 (d,  $J=7.81$  Hz, 2H), 7.36 (d,  $J=8.52$  Hz, 4H), 7.20 ppm (t,  $J=7.18$  Hz, 4H); MS (ESI+):  $m/z=581.02$  [ $M+H$ ] $^+$ ; elemental analysis: calcd (%) for  $C_{26}H_{18}Cl_2N_6O_2Zn$ : C 53.59, H 3.11, N 14.42; found: C 53.61, H 3.12, N 14.48.

**3**: White solid (78%) soluble in CH<sub>2</sub>Cl<sub>2</sub>. <sup>1</sup>H NMR (CDCl<sub>3</sub>):  $\delta=8.31$  (s, 2H), 8.03 (d,  $J=4.64$  Hz, 2H), 7.75 (t,  $J=7.63$  Hz, 2H), 7.35 (d,  $J=7.71$  Hz, 2H), 7.20 (t,  $J=7.13$  Hz, 2H), 2.41 (t,  $J=7.71$  Hz, 4H), 1.70–1.59 (m, 4H), 1.26–1.21 (m, 16H), 0.85 ppm (t,  $J=6.84$  Hz, 6H); MS (ESI+):  $m/z=557.25$  [ $M+H$ ] $^+$ ; elemental analysis: calcd (%) for  $C_{28}H_{40}N_6O_2Zn$ : C 60.26, H 7.22, N 15.06; found: C 60.21, H 7.30, N 15.11.

**4**: White solid (80%) soluble in CH<sub>2</sub>Cl<sub>2</sub>. <sup>1</sup>H NMR (CDCl<sub>3</sub>):  $\delta=8.27$  (s, 2H), 7.76 (s, 2H), 7.30 (d,  $J=7.63$  Hz, 2H), 7.21 (t,  $J=7.72$  Hz, 2H), 3.91 (t,  $J=6.63$  Hz, 4H), 2.40 (t,  $J=7.23$  Hz, 4H), 1.88–1.71 (m, 8H), 1.71–1.48 (m, 4H), 1.49–1.28 (m, 28H), 1.25–1.20 (m, 12H), 0.92–0.85 ppm (m, 12H); MS (ESI+):  $m/z=869.55$  [ $M+H$ ] $^+$ ; elemental analysis: calcd (%) for  $C_{48}H_{80}N_6O_4Zn$ : C 66.22, H 9.26, N 9.65; found: C 65.99, H 9.19, N 9.66.

**5**: Yellow solid (71%) soluble in CH<sub>2</sub>Cl<sub>2</sub>. <sup>1</sup>H NMR (CDCl<sub>3</sub>):  $\delta=8.60$  (s, 2H), 8.24 (d,  $J=8.43$  Hz, 2H), 7.71 (d,  $J=8.32$  Hz, 4H), 7.58–7.51 (m, 4H), 7.40 (t,  $J=7.17$  Hz, 2H), 2.33 (t,  $J=7.87$  Hz, 4H), 1.70–1.60 (m, 4H), 1.30–1.18 (m, 16H), 0.82 ppm (t,  $J=7.77$  Hz, 6H); MS (ESI+):  $m/z=657.28$  [ $M+H$ ] $^+$ ; elemental analysis: calcd (%) for  $C_{36}H_{44}N_6O_2Zn$ : C 65.70, H 6.74, N 12.77; found: C 65.86, H 6.80, N 12.69.

**6**: Yellow solid (91%) soluble in CH<sub>2</sub>Cl<sub>2</sub>. <sup>1</sup>H NMR (CDCl<sub>3</sub>):  $\delta=8.47$  (s, 2H), 8.20 (d,  $J=8.66$  Hz, 4H), 8.02 (d,  $J=4.30$  Hz, 2H), 7.69 (t,  $J=7.20$  Hz, 2H), 7.33 (d,  $J=7.70$  Hz, 2H), 7.10 (t,  $J=5.02$  Hz, 2H), 6.88 (d,  $J=8.66$  Hz, 4H), 3.82 ppm (s, 6H); MS (ESI+):  $m/z=573.12$  [ $M+H$ ] $^+$ ; elemental analysis: calcd (%) for  $C_{28}H_{24}N_6O_4Zn \cdot H_2O$ : C 56.81, H 4.43, N 14.20; found: C 56.77, H 4.44, N 14.18.

**7**: Yellow solid (88%) soluble in CH<sub>2</sub>Cl<sub>2</sub>. <sup>1</sup>H NMR (CDCl<sub>3</sub>):  $\delta=8.41$  (s, 2H), 8.18 (d,  $J=8.90$  Hz, 4H), 7.75 (s, 2H), 7.23 (d,  $J=8.60$  Hz, 2H), 7.12 (d,  $J=8.66$  Hz, 2H), 6.87 (d,  $J=8.96$  Hz, 4H), 3.87 (s, 6H), 3.85–3.75 (m, 4H), 1.69–1.59 (m, 4H), 1.30–1.20 (m, 28H), 0.88 ppm (t,  $J=6.77$  Hz, 6H); MS (ESI+):  $m/z=885.42$  [ $M+H$ ] $^+$ ; elemental analysis: calcd (%) for  $C_{48}H_{64}N_6O_6Zn \cdot H_2O$ : C 63.74, H 7.36, N 9.29; found: C 63.79, H 7.44, N 9.21.

**8**: Yellow solid (85%) soluble in CH<sub>2</sub>Cl<sub>2</sub>. <sup>1</sup>H NMR (CDCl<sub>3</sub>):  $\delta=8.81$  (s, 2H), 8.22 (d,  $J=8.43$  Hz, 2H), 8.13 (d,  $J=8.83$  Hz, 4H), 7.77 (d,  $J=8.69$  Hz, 2H), 7.68 (d,  $J=7.04$  Hz, 2H), 7.63 (d,  $J=8.52$  Hz, 2H), 7.46 (t,  $J=7.24$  Hz, 2H), 7.35 (t,  $J=7.41$  Hz, 2H), 6.82 (d,  $J=8.92$  Hz, 4H), 3.80 ppm (s, 6H); MS (ESI+):  $m/z=673.15$  [ $M+H$ ] $^+$ ; elemental analysis: calcd (%) for  $C_{36}H_{28}N_6O_4Zn$ : C 64.15, H 4.19, N 12.47; found: C 64.33, H 4.13, N 12.52.

**9**: Dark-brown solid (85%) soluble in MeOH. <sup>1</sup>H NMR (CD<sub>3</sub>OD/CDCl<sub>3</sub>=1:1 v/v):  $\delta=208.80$ , 63.76, 33.00, 32.76, 29.87, 7.58, 6.86, 4.66, 4.07, 3.50, 3.34, 2.20, 1.18, –0.87, –2.88, –65.27 ppm; MS (ESI+):  $m/z=668.15$  [ $M+H$ ] $^+$ ; elemental analysis: calcd (%) for  $C_{36}H_{28}CoN_6O_4 \cdot CH_3OH$ : C 63.52, H 4.61, N 12.01; found: C 63.44, H 4.71, N 11.89.

**10**: Yellowish-brown solid (85%) soluble in MeOH/CHCl<sub>3</sub>. <sup>1</sup>H NMR (CD<sub>3</sub>OD/CDCl<sub>3</sub>=1:1 v/v):  $\delta=47.50$ , 25.68, 13.98, 13.72, 9.66, 7.48, 7.27,

5.26, 4.74, 4.08, 3.61, 3.34, 1.24, 1.18, 0.85, 0.08 ppm; MS (ESI+):  $m/z=667.16$  [ $M+H$ ] $^+$ ; elemental analysis: calcd (%) for  $C_{36}H_{28}N_6NiO_4 \cdot H_2O$ : C 63.09, H 4.41, N 12.26; found: C 63.00, H 4.47, N 12.30.

**11**: Yellow solid (95%) soluble in CH<sub>2</sub>Cl<sub>2</sub>. <sup>1</sup>H NMR (CDCl<sub>3</sub>):  $\delta=8.79$  (s, 2H), 8.25 (d,  $J=8.40$  Hz, 2H), 8.18 (d,  $J=8.85$  Hz, 4H), 7.77 (d,  $J=8.54$  Hz, 2H), 7.70 (d,  $J=7.64$  Hz, 2H), 7.58 (d,  $J=8.43$  Hz, 2H), 7.51 (t,  $J=7.80$  Hz, 2H), 7.37 (t,  $J=7.52$  Hz, 2H), 6.86 (d,  $J=8.90$  Hz, 4H), 3.82 ppm (s, 6H); MS (ESI+):  $m/z=723.13$  [ $M+H$ ] $^+$ ; elemental analysis: calcd (%) for  $C_{36}H_{28}CdN_6O_4$ : C 59.97, H 3.91, N 11.66; found: C 59.89, H 3.88, N 11.58.

**2**: A mixture of **L7** (0.3 mmol) and Zn(SO<sub>4</sub>)·7H<sub>2</sub>O (0.3 mmol) was stirred in MeOH/MeCN (1:1 v/v, 30.0 mL) at room temperature under N<sub>2</sub> for 4 h. **L8** (0.3 mmol) and Na<sub>2</sub>CO<sub>3</sub> (0.66 mmol) were then added to the mixture, which was further stirred for another 4 h. The crude product obtained was purified by flash chromatography. Heteroligand zinc complex **2** (30%) was obtained as shiny yellow crystals. <sup>1</sup>H NMR (CDCl<sub>3</sub>):  $\delta=8.66$  (s, 1H), 8.38 (s, 1H), 8.16 (d,  $J=8.82$  Hz, 2H), 8.12 (d,  $J=8.86$  Hz, 1H), 7.76–7.70 (m, 2H), 7.66–7.59 (m, 2H), 7.52 (d,  $J=8.40$  Hz, 1H), 7.44 (t,  $J=7.65$  Hz, 1H), 7.26 (d,  $J=7.55$  Hz, 1H), 7.06 (d,  $J=8.53$  Hz, 1H), 6.85 (d,  $J=8.85$  Hz, 2H), 3.77 (t,  $J=7.40$  Hz, 2H), 3.75 (s, 3H), 2.17 (s, 3H), 1.66–1.57 (m, 2H), 1.38–1.26 (m, 14H), 0.88 ppm (t,  $J=6.73$  Hz, 3H); MS (ESI+):  $m/z=687.26$  [ $M+H$ ] $^+$ ; elemental analysis: calcd (%) for  $C_{36}H_{42}N_6O_4Zn$ : C 62.83, H 6.15, N 12.21; found: C 63.00, H 6.24, N 12.12.

General procedure for the preparation of the neutral metallosupramolecular polymers: The self-assembly reaction was performed by adding the carboxaldehyde (Py2al, Py2alC<sub>10</sub>, or Qui2al; 0.3 mmol), polydimethylsiloxane- $\alpha,\omega$ -hydrazide (**BH1** or **BH2**; 0.15 mmol), transition-metal salt (Co<sup>II</sup>, Ni<sup>II</sup>, Zn<sup>II</sup>, or Cd<sup>II</sup>; 0.15 mmol), Na<sub>2</sub>CO<sub>3</sub> (0.33 mmol), and anhydrous Na<sub>2</sub>SO<sub>4</sub> (3 mmol) to a mixture of MeOH and CH<sub>2</sub>Cl<sub>2</sub> (1:1 v/v, 0.15 mmol). The reaction mixture was stirred at room temperature under N<sub>2</sub> for 24 h. The solution was then evaporated to dryness, and CH<sub>2</sub>Cl<sub>2</sub> was added to redissolve the mixture. Na<sub>2</sub>CO<sub>3</sub> and Na<sub>2</sub>SO<sub>4</sub> were filtered off. A polymer film was obtained by casting in a petri dish (2.5 cm diameter), redissolving the polymer product in CH<sub>2</sub>Cl<sub>2</sub>, and then letting the solution slowly evaporate under ambient atmosphere and at 50 °C.

**P1** (Zn<sup>II</sup>-Py2al-**BH1**):  $M_r \approx 33\,000$  g mol<sup>–1</sup>; <sup>1</sup>H NMR (25 mM, CDCl<sub>3</sub>):  $\delta=8.31$  (s, 2H), 8.02 (d,  $J=4.54$  Hz, 2H), 7.74 (t,  $J=7.59$  Hz, 2H), 7.35 (d,  $J=7.72$  Hz, 2H), 7.20 (t,  $J=7.43$  Hz, 2H), 2.42 (t,  $J=7.73$  Hz, 4H), 1.70–1.60 (m, 4H), 1.46–1.26 (m, 4H), 0.59–0.49 (m, 4H), 0.10 ppm (s, 90H).

**P2** (Zn<sup>II</sup>-Py2alC<sub>10</sub>-**BH1**):  $M_r \approx 39\,000$  g mol<sup>–1</sup>; <sup>1</sup>H NMR (25 mM, CDCl<sub>3</sub>):  $\delta=8.27$  (s, 2H), 7.76 (s, 2H), 7.30–7.21 (m, 2H), 7.17 (br, 2H), 3.91 (t,  $J=6.61$  Hz, 4H), 2.40 (br, 4H), 1.85–1.73 (m, 8H), 1.49–1.28 (m, 32H), 0.89 (br, 6H), 0.60–0.49 (m, 4H), 0.10 ppm (s, 90H).

**P3** (Zn<sup>II</sup>-Qui2al-**BH1**):  $M_r \approx 43\,000$  g mol<sup>–1</sup>; <sup>1</sup>H NMR (25 mM, CDCl<sub>3</sub>):  $\delta=8.61$  (s, 2H), 8.23 (d,  $J=8.45$  Hz, 2H), 7.71 (d,  $J=8.35$  Hz, 4H), 7.58–7.51 (m, 4H), 7.40 (t,  $J=7.08$  Hz, 2H), 2.36 (t,  $J=7.87$  Hz, 4H), 1.65–1.45 (m, 4H), 1.30–1.17 (m, 4H), 0.50–0.37 (m, 4H), 0.10 ppm (s, 90H).

**P4** (Zn<sup>II</sup>-Py2al-**BH2**):  $M_r \approx 55\,000$  g mol<sup>–1</sup>; <sup>1</sup>H NMR (25 mM, CDCl<sub>3</sub>):  $\delta=8.49$  (s, 2H), 8.19 (d,  $J=8.76$  Hz, 4H), 8.00 (d,  $J=8.36$  Hz, 2H), 7.76–7.65 (m, 2H), 7.40–7.31 (m, 2H), 7.18–7.08 (m, 2H), 6.88 (d,  $J=8.76$  Hz, 4H), 4.05 (t,  $J=6.46$  Hz, 4H), 1.85 (t,  $J=7.3$  Hz, 4H), 1.58–1.35 (m, 8H), 0.66–0.54 (m, 4H), 0.10 ppm (s, 90H).

**P5** (Zn<sup>II</sup>-Py2alC<sub>10</sub>-**BH2**):  $M_r \approx 38\,000$  g mol<sup>–1</sup>; <sup>1</sup>H NMR (25 mM, CDCl<sub>3</sub>):  $\delta=8.43$  (s, 2H), 8.18 (d,  $J=8.62$  Hz, 4H), 7.76 (s, 2H), 7.25 (d,  $J=8.60$  Hz, 2H), 7.13 (d,  $J=7.66$  Hz, 2H), 6.87 (d,  $J=8.90$  Hz, 4H), 4.13–4.04 (m, 4H), 3.81 (br, 4H), 2.45–2.30 (m, 4H), 1.90–1.72 (m, 4H), 1.49–1.28 (m, 36H), 0.89 (t,  $J=6.97$  Hz, 6H), 0.64–0.54 (m, 4H), 0.10 ppm (s, 90H).

**P6** (Zn<sup>II</sup>-Qui2al-**BH2**):  $M_r \approx 45\,000$  g mol<sup>–1</sup>; <sup>1</sup>H NMR (25 mM, CDCl<sub>3</sub>):  $\delta=8.80$  (s, 2H), 8.21 (d,  $J=8.60$  Hz, 2H), 8.13 (br, 4H), 7.76 (d,  $J=8.14$  Hz, 2H), 7.67 (d,  $J=7.64$  Hz, 2H), 7.60 (d,  $J=8.73$  Hz, 2H), 7.49–7.41 (m, 2H), 7.37–7.31 (m, 2H), 6.80 (d,  $J=8.19$  Hz, 4H), 3.92 (br, 4H), 1.80 (br, 4H), 1.48–1.37 (m, 8H), 0.65–0.50 (m, 4H), 0.11 ppm (s, 90H).

**P7** (Co<sup>II</sup>-Qui2al-**BH2**): <sup>1</sup>H NMR (25 mM, CD<sub>3</sub>OD/CDCl<sub>3</sub>=1:1 v/v):  $\delta=208.83$ , 63.54, 33.07, 32.98, 29.89, 7.56, 6.91, 4.66, 4.10, 3.34, 3.34, 2.25, 2.12, 1.23, 0.60, 0.43, 0.32, –0.87, 0.06, –0.01, –0.05, –0.08, –0.16, –0.21,

−0.24, −0.29, −0.36, −0.40, −0.86, −2.78, −65.22, 57.95, 57.69, 32.96, 32.76, 29.41, 7.62, 5.37, 5.34, 5.27, 2.58, 2.46, 2.07, 1.30, 0.67, 0.55, 0.11, 0.06, 0.04, 0.00 ppm.

**P8** (Ni<sup>II</sup>-Qui2al-BH2): <sup>1</sup>H NMR (25 mM, CD<sub>3</sub>OD/CDCl<sub>3</sub> = 1:1 v/v): δ = 47.38, 25.61, 13.94, 13.63, 9.66, 7.48, 7.23, 6.88, 5.33, 4.49, 3.98, 3.68, 3.34, 1.77, 1.57, 1.41, 1.26, 0.85, 0.79, 0.56, 0.43, 0.06, −0.03 ppm.

**P9** (Cd<sup>II</sup>-Qui2al-BH2): *M<sub>n</sub>* ≈ 52 000 g mol<sup>−1</sup>; <sup>1</sup>H NMR (25 mM, CDCl<sub>3</sub>): δ = 8.80 (s, 2H), 8.26 (d, *J* = 8.71 Hz, 2H), 8.17 (d, *J* = 7.72 Hz, 4H), 7.77 (d, *J* = 8.41 Hz, 2H), 7.71 (d, *J* = 7.65 Hz, 2H), 7.60 (d, *J* = 8.11 Hz, 2H), 7.51 (br, 2H), 7.38 (t, *J* = 7.11 Hz, 2H), 6.85 (d, *J* = 8.52 Hz, 4H), 3.97 (br, 4H), 1.76 (br, 4H), 1.46–1.39 (m, 8H), 0.65–0.51 (m, 4H), 0.11 (s, 90H).

Polymer formation from combinatorial-subunit selection driven by zinc(II) metal ion: The self-assembly reaction was performed by adding Py2al (0.3 mmol), benzaldehyde (0.3 mmol), 3-chloro-4-pyridinecarboxaldehyde (0.3 mmol), 2-methoxy-3-pyridinecarboxaldehyde (0.3 mmol), **BH1** (0.15 mmol), Na<sub>2</sub>CO<sub>3</sub> (0.33 mmol), and anhydrous Na<sub>2</sub>SO<sub>4</sub> (3 mmol) to MeOH/CH<sub>2</sub>Cl<sub>2</sub> (1:1 v/v, 15.0 mL) with a) 0 mmol and b) 0.3 mmol of Zn(SO<sub>4</sub>)·7H<sub>2</sub>O. The reaction mixture was stirred at 25 °C under N<sub>2</sub> for 24 h. The solution was then evaporated. CH<sub>2</sub>Cl<sub>2</sub> was added to redissolve the crude mixture, and Na<sub>2</sub>CO<sub>3</sub> and Na<sub>2</sub>SO<sub>4</sub> were removed by filtration. The solution was then evaporated again. The resulting mixture was analyzed by <sup>1</sup>H NMR spectroscopy in CDCl<sub>3</sub> (1.00 mL).

Dynamic properties of **P1** at different concentrations, time, and temperature in CDCl<sub>3</sub>: The average molecular weight of polymer **P1** was determined by integration of the <sup>1</sup>H NMR signals for the imine CH or OCH<sub>2</sub> protons at uncomplexed and complexed coordination sites and used to reveal the dynamic behavior of **P1**. Different concentrations (50.00, 25.00, 12.50, 6.25, and 3.125 mM) of **P1** in CDCl<sub>3</sub> were prepared. The five samples were kept at 25 °C. At different time periods (0, 12, 24, and 48 h), <sup>1</sup>H NMR spectroscopic analysis of these samples were conducted.

## Acknowledgements

We thank Dr. André de Cian for helping with X-ray diffraction crystallography and Mitsui Chemical, Inc. for conducting differential scanning calorimetry and elastic modulus measurements. C.-F.C. acknowledges a postdoctoral fellowship from the Croucher Foundation, Hong Kong.

- [1] a) J.-M. Lehn in *Supramolecular Science: Where It Is and Where It Is Going* (Eds.: R. Ungaro, E. Dalcaneale), Kluwer, Dordrecht, **1999**, pp. 287–304; b) J.-M. Lehn, *Proc. Natl. Acad. Sci. USA* **2002**; c) J.-M. Lehn, *Chem. Soc. Rev.* **2007**, *36*, 151–160.
- [2] a) J.-M. Lehn, *Chem. Eur. J.* **1999**, *5*, 2455–2463; b) J.-M. Lehn, A. V. Eliseev, *Science* **2001**, *291*, 2331–2332; c) S. J. Rowan, S. J. Cantrill, G. R. L. Cousins, J. K. M. Sanders, J. F. Stoddart, *Angew. Chem.* **2002**, *114*, 938–993; *Angew. Chem. Int. Ed.* **2002**, *41*, 898–952; d) P. T. Corbett, J. Leclaire, L. Vial, K. R. West, J.-L. Wietor, J. K. M. Sanders, S. Otto, *Chem. Rev.* **2006**, *106*, 3652–3711.
- [3] a) J.-M. Lehn, *Makromol. Chem. Macromol. Symp.* **1993**, *69*, 1–17; b) L. Brunsveld, B. J. Folmer, E. W. Meijer, R. P. Sijbesma, *Chem. Rev.* **2001**, *101*, 4071–4197; c) J.-M. Lehn, *Polym. Int.* **2002**, *51*, 825–839; d) *Supramolecular Polymers*, 2nd ed. (Ed.: A. Ciferri), Taylor & Francis, Boca Raton, **2005**; e) J.-M. Lehn, *Prog. Polym. Sci.* **2005**, *30*, 814–831.
- [4] *Contemporary Polymer Chemistry*, 2nd ed. (Eds.: H. R. Allcock, F. W. Lampe), Prentice Hall, London, **1990**.
- [5] a) W. G. Skene, J.-M. Lehn, *Proc. Natl. Acad. Sci. USA* **2004**, *101*, 8270–8275; b) X. Chen, M. A. Dam, K. Ono, A. Mal, H. Shen, S. R. Nutt, K. Sheran, F. Wudl, *Science* **2002**, *295*, 1698–1702; c) H. Otsuka, K. Aotani, Y. Higaki, A. Takahara, *Chem. Commun.* **2002**, 2838–2839; d) H. Otsuka, K. Aotani, Y. Higaki, A. Takahara, *J. Am. Chem. Soc.* **2003**, *125*, 4064–4065; e) G. Yamaguchi, Y. Higaki, H. Otsuka, A. Takahara, *Macromolecules* **2005**, *38*, 6316–6320; f) T. Ono, T. Nobori, J.-M. Lehn, *Chem. Commun.* **2005**, 1522–1524; g) N. Giuseppone, G. Fuks, J.-M. Lehn, *Chem. Eur. J.* **2006**, *12*, 1723–1735; h) T. Ono, S. Fujii, T. Nobori, J.-M. Lehn, *Chem. Commun.* **2007**, 46–48; i) T. Ono, S. Fujii, T. Nobori, J.-M. Lehn, *Chem. Commun.* **2007**, 4360–4362; j) D. Sheba, F. Wudl, *J. Mater. Chem.* **2008**, *18*, 41–62.
- [6] a) R. Dobrawa, F. Wurthner, *J. Polym. Sci. Part A* **2005**, *43*, 4981–4995; b) H. Hofmeier, R. Hoogenboom, M. E. L. Wouters, U. S. Schubert, *J. Am. Chem. Soc.* **2005**, *127*, 2913–2921; c) H. Hofmeier, U. S. Schubert, *Chem. Commun.* **2005**, 2423–2432; d) J. B. Beck, J. Ineman, M. S. J. Rowan, *Macromolecules* **2005**, *38*, 5060–5068; e) H. Hofmeier, A. El-ghayoury, A. P. H. J. Schenning, U. S. Schubert, *Chem. Commun.* **2004**, 318–319; f) P. R. Andres, U. S. Schubert, *Adv. Mater.* **2004**, *16*, 1043–1068; g) J.-F. Gohy, B. G. G. Lohmeijer, U. S. Schubert, *Chem. Eur. J.* **2003**, *9*, 3472–3479; h) H. Hofmeier, S. Schmatloch, D. Wouters, U. S. Schubert, *Macromol. Chem. Phys.* **2003**, *204*, 2197–2203; i) J. B. Beck, S. J. Rowan, *J. Am. Chem. Soc.* **2003**, *125*, 13922–13923; j) U. S. Schubert, C. Eschbaumer, *Angew. Chem.* **2002**, *114*, 3016–3050; *Angew. Chem. Int. Ed.* **2002**, *41*, 2892–2926; k) S. Schmatloch, M. Fernandez-González, U. S. Schubert, *Macromol. Rapid Commun.* **2002**, *23*, 957–961.
- [7] C. F. Chow, S. Fujii, J.-M. Lehn, *Angew. Chem.* **2007**, *119*, 5095–5098; *Angew. Chem. Int. Ed.* **2007**, *46*, 5007–5010.
- [8] a) J. R. Nitschke, J.-M. Lehn, *Proc. Natl. Acad. Sci. USA* **2003**, *100*, 11970–11974; b) J. R. Nitschke, *Acc. Chem. Res.* **2007**, *40*, 103–112.
- [9] U. S. Schubert, H. Hofmeier, G. R. Newkome, *Modern Terpyridine Chemistry*, Wiley-VCH, Weinheim, **2006**.
- [10] a) M. Ruben, J.-M. Lehn, G. Vaughan, *Chem. Commun.* **2003**, 1338–1339; b) L. H. Uppadine, J.-P. Gisselbrecht, J.-M. Lehn, *Chem. Commun.* **2004**, 718–719; c) L. H. Uppadine, J.-P. Gisselbrecht, N. Kyritsakas, K. Nattinen, K. Rissanen, J.-M. Lehn, *Chem. Eur. J.* **2005**, *11*, 2549–2565.
- [11] a) C. M. Armstrong, P. V. Bernhardt, P. Chin, D. R. Richardson, *Eur. J. Inorg. Chem.* **2003**, 1145–1156; b) X. Y. Cao, N. Kyritsakas-Gruber, J. Harrowfield, A. Madalan, J. R. Nitschke, J. Ramirez, K. Rissanen, L. Russo, A.-M. Stadler, G. Vaughan, J.-M. Lehn, *Eur. J. Inorg. Chem.* **2007**, 2944–2965.
- [12] Crystallographic data for complex **1** are described in the Supporting Information.
- [13] A comparison of the <sup>1</sup>H NMR spectroscopic data of neutral model homoligand complexes **3–11** and metallosupramolecular polymers **P1–P9** is described in the Supporting Information.
- [14] a) A. Ciferri, *Macromol. Rapid Commun.* **2002**, *23*, 511–529; b) F. Würthner, C. Thalacker, A. Sautter, W. Schärfl, W. Ibach, O. Hollricher, *Chem. Eur. J.* **2000**, *6*, 3871–3886.
- [15] a) E. J. Blanz, F. A. Frence, Jr., J. R. Do Amaral, D. A. French, *J. Med. Chem.* **1970**, *13*, 1124–1130; b) B. Kang, M. Kim, J. Lee, Y. Do, S. Chang, *J. Org. Chem.* **2006**, *71*, 6721–6727.

Received: March 14, 2008